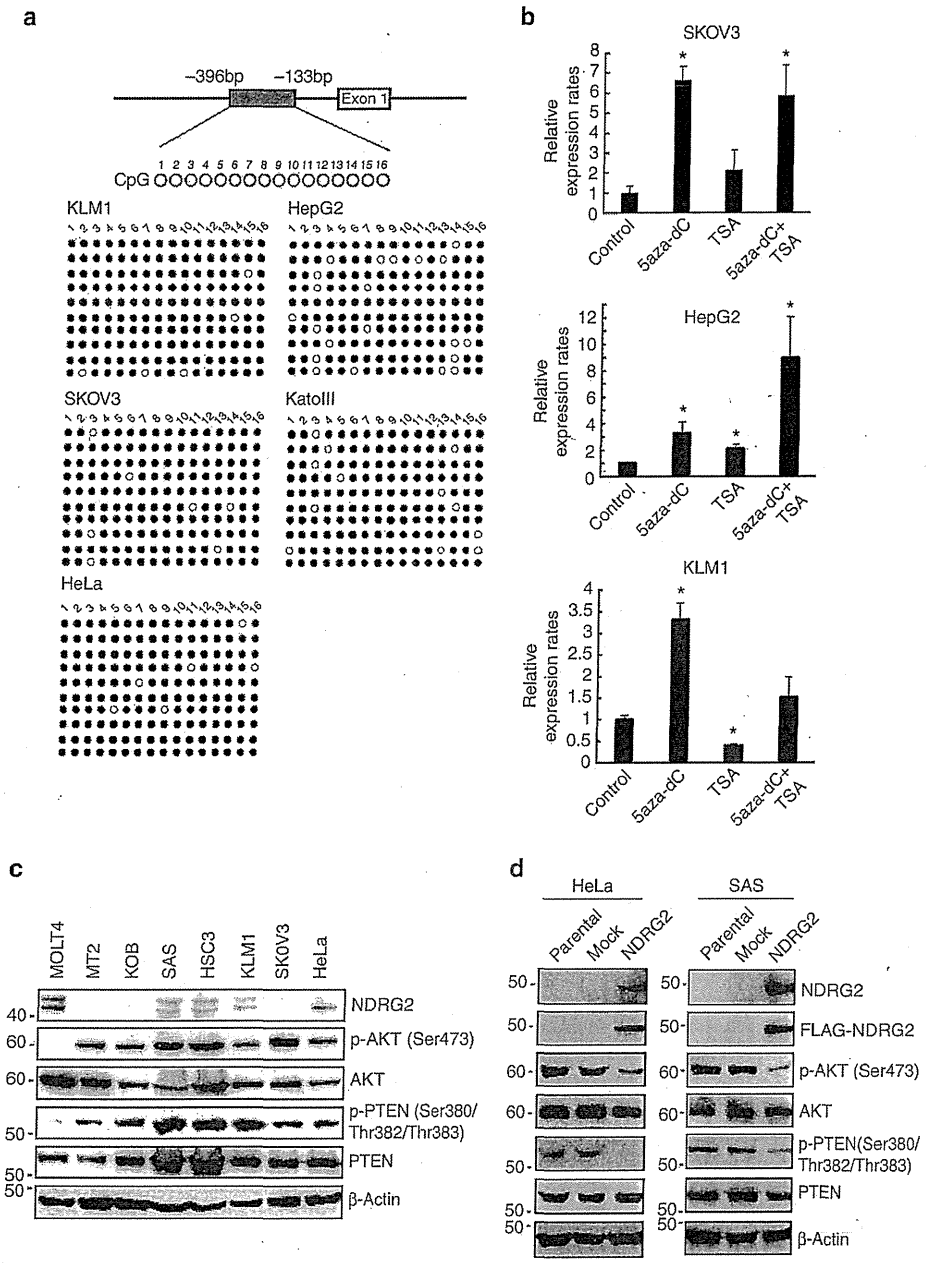

Figure 7 | Downregulation of NDRG2 is associated with enhanced phosphorylation of PTEN-Ser380/Thr382/Thr383 and enhanced activation of PI3K-AKT in various cancers. (**a**) Bisulfite genomic sequencing of the *NDRG2* promoter region in the KLM1 (pancreatic cancer), SKOV3 (ovarian cancer), HeLa (cervical cancer), HepG2 (hepatic cancer) and KatoIII (gastric cancer) cell lines. PCR products amplified from bisulfite-treated genomic DNA were subcloned, and ten clones in each cell line were sequenced. Open circles indicate unmethylated CpGs (Thy) and filled circles indicate methylated CpGs (Cyt). The region sequenced spans from −396 bp to −133 bp. (**b**) SKOV3, HepG2 and KLM1 cells were cultured with 10 μM 5-aza-dC for 72 h, with 1.2 μM TSA for 48 h, or with 1.2 μM of TSA for 48 h, followed by 10 μM of 5-aza-dC for 24 h. After treatments, total RNA was extracted and quantitative RT-PCR was performed with *NDRG2* and β-actin. The relative amounts of mRNA were normalized against β-actin mRNA and expressed relative to the mRNA abundance in untreated cells. The mean ± s.d. is shown; $*P<0.05$ compared with the untreated control (Student's *t*-test). The data are representative of two experiments. (**c**) Western blot analyses of NDRG2, PTEN, p-PTEN (Ser380/Thr382/Thr383), AKT and p-AKT (Ser473) were performed in SAS (OSCC), HSC3 (OSCC), KLM1, SKOV3, HeLa, MT2 (ATLL), KOB (ATLL) and MOLT4 (T-ALL) cell lines. The data are representative of two experiments. (**d**) HeLa and SAS cells stably transfected with Mock or FLAG-NDRG2 expression vector were subjected to western blotting. The data are representative of three experiments.

Discussion

In this study, we show that NDRG2 interacts with PTEN and promotes its dephosphorylation at Ser380/Thr382/Thr383 by recruiting PP2A to PTEN. We also demonstrated that loss of *NDRG2* expression via genetic or epigenetic abnormalities in ATLL cells can contribute to the increase in PTEN-Ser380/Thr382/Thr383 phosphorylation, which leads to inactivation of PTEN lipid phosphatase activity and activation of the PI3K-AKT

pathway. The imbalance of the expression of *NDRG2* and as yet unidentified protein kinases might account for an elevation of PTEN-Ser380/Thr382/Thr383 phosphorylation with a high amount of phosphorylated AKT in ATLL cells. Finally, we showed that *NDRG2*-deficient mice develop multiple types of tumours, thus establishing that loss of *NDRG2* expression can contribute to tumour development.

PTEN stability and lipid phosphatase activity can be regulated through phosphorylation of the C-terminal tail, which contains a cluster of serine–threonine residues: Ser370, Ser380, Thr382, Thr383 and Ser385 (ref. 35). Although the cluster of Ser380/Thr382/Thr383 residues in the C-terminal tail are thought to be minor phosphorylation sites[26,36], the level of phosphorylated PTEN-Ser380/Thr382/Thr383 has been shown to be rapidly and transiently increased in hypothalamic cells treated with leptin and in rat brains following transient middle cerebral artery occlusion[37,38]. CK2 is known to be a major kinase that phosphorylates PTEN at the C-terminal serine–threonine cluster, but phosphorylation of Ser380/Thr382/Thr383 by CK2 is still under debate[21,26,36,39]. We observed that suppression of CK2 activity with specific inhibitors in ATLL cells did not influence PTEN-Ser380/Thr382/Thr383 phosphorylation. Thus, it is likely that CK2 is not responsible for the phosphorylation of PTEN at Ser380/Thr382/Thr383 in ATLL cells. In contrast, the expression of NDRG2 is markedly upregulated in several tumour cell lines exposed to hypoxic conditions and is thought to be a new hypoxia-inducible factor-1 target gene[40,41]. It could be speculated that *NDRG2* expression is induced by hypoxia-ischemia in the brain to regulate PTEN phosphorylation, leading to the suppression of PI3K-AKT activation and induction of apoptosis. Interestingly, several kinases, including SGK1 (serum- and glucocorticoid-induced kinase 1), PKCθ (protein kinase C-θ) and AKT, have been found to phosphorylate NDRG2 (refs 42,43). These phosphorylation events are likely to affect the cellular function of NDRG2. It is intriguing to speculate that NDRG2 might be a downstream target of the PI3K-AKT signalling pathway that may participate in a negative feedback loop in PI3K-AKT signalling. PP2A exists predominantly as a heterotrimer composed of catalytic C, structural A and one member of four families of regulatory B subunits. The activity, substrate specificity and subcellular localization of the PP2A holoenzyme are thought to be determined by its B subunit[44]. A recent study has shown that following AKT phosphorylation, Clk2 is activated and phosphorylates the PP2A regulatory subunit B56β, thereby leading to the assembly of the PP2A holoenzyme complex on AKT and dephosphorylation of AKT at both Thr308 and Ser473 (ref. 45). Thus, a more complex feedback regulation governing NDRG2 and PP2A activities may exist within the PI3K-AKT pathway. Identifying the PP2A regulatory subunit that interacts with NDRG2 would provide important clues in understanding how the dephosphorylation of PTEN by NDRG2-PP2A is regulated upon AKT activation.

Elevated phosphorylation of PTEN-Ser380/Thr382/Thr383 with high levels of activated AKT is frequently observed in acute myeloid leukaemia (AML) and is associated with poor prognosis[46]. The phosphorylation of Ser380/Thr382/Thr383 is also elevated in human fibromyomatous uteri and may be a contributory factor in the development of uterine leiomyomas[47]. Although it is not known whether these phosphorylation events are attributed to the functional inactivation of *NDRG2*, decreased expression and promoter methylation of the *NDRG2* gene have been reported in various types of cancer, such as liver cancers, gastric cancers, colon cancers and glioblastomas[30,31,48–51]. Therefore, we hypothesize that in ATLL and other types of tumour cells without genetic alterations in the PI3K-AKT pathway, the suppression of *NDRG2* transcription disrupts the negative regulation of PI3K-AKT signalling via sustained PTEN-Ser380/Thr382/Thr383 phosphorylation during tumour development (Fig. 8). The finding that PTEN-Ser380/Thr382/Thr383 is highly phosphorylated in all of the organs of *NDRG2*-deficient mice provides additional evidence that the balance between an unidentified PTEN-Ser380/Thr382/Thr383 kinase(s) and PP2A-NDRG2 activity regulates the phosphorylation status of PTEN-Ser380/Thr382/Thr383 *in vivo*. Therefore, we are currently attempting to identify the protein kinase(s) that target PTEN-Ser380/Thr382/Thr383, which has the potential to be a therapeutic drug target in a variety of cancers, including ATLL.

Because NDRG2 has been shown to have growth inhibitory effects on several malignant cell lines through downregulation of several signalling pathways, including PI3K-AKT, janus kinase-signal transducer and activator of transcription (JAK-STAT) and nuclear factor-kappaB signalling[52,53], one may speculate that the phosphorylation of different proteins involved in these signalling pathways is regulated by the PP2A-NDRG2 complex. Indeed, we observed that the ectopic expression of NDRG2 in ATLL cells causes suppression of JAK-STAT and nuclear factor-kappaB activation (data not shown), although the molecular mechanisms underlying these effects are still being elucidated. We speculate that NDRG2 may have a key role in suppressing different oncogenic signalling pathways in tumourigenesis. In conclusion, this study provides the first functional evidence for a tumour suppressor role of NDRG2 and suggests that NDRG2 is involved in the leukaemogenesis of ATLL. Further investigations of the

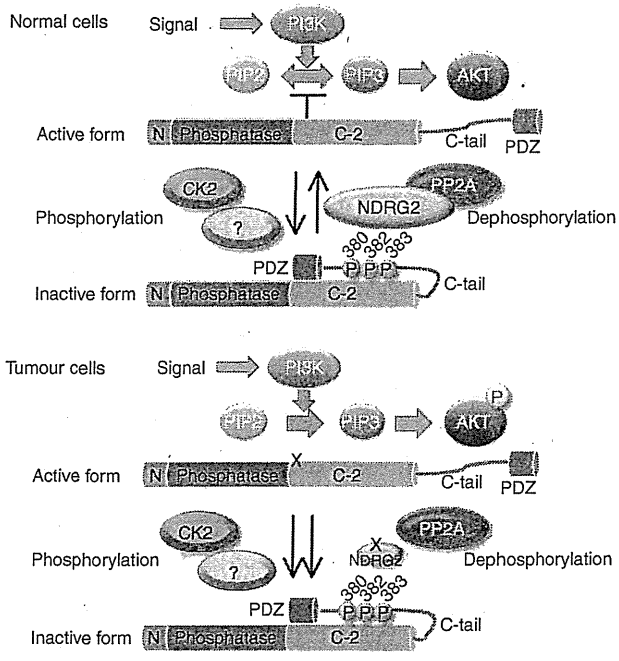

Figure 8 | Schematic model for the regulation of PTEN activity by NDRG2. In normal cells, PP2A is efficiently recruited to PTEN via its interaction with NDRG2, which may facilitate dephosphorylation of PTEN at Ser380/Thr382/Thr383, resulting in an active open conformation of PTEN and subsequently leading to the dephosphorylation of PIP_3 to PIP_2. In tumour cells, expression of NDRG2 is inhibited by DNA methylation of its promoter, causing sustained phosphorylation of PTEN, which keeps PTEN in an inactive closed conformation. Loss of PTEN activity leads to increased PIP_3 levels and AKT activation. The balance between the expression of NDRG2 and an unidentified kinase(s) may have an important role in regulating the phosphorylation status of PTEN.

roles of NDRG2 in the regulation of different signalling pathways may provide clues in understanding the underlying mechanisms of cancer.

Methods

Cell lines. Jurkat, MOLT4, KAWAI and MKB1 are HTLV-1-negative human T-ALL cell lines. KOB, SO4 and KK1 are IL2-dependent ATLL cell lines. ED, Su9T-01 and S1T are IL2-independent ATLL cell lines. MT2, MT4 and HUT102 are human T-cell lines transformed by HTLV-1 infection. Jurkat, MOLT4 and MKB1 were obtained from the Fujisaki Cell Center, Hayashibara Biochemical Laboratories (Okayama, Japan). KAWAI was kindly provided by Dr Y. Hayashi (Gunma Children's Medical Center, Gunma, Japan). MT2, MT4 and HUT102 were kind gifts from Dr H. Iha (Oita University, Oita, Japan). KOB, SO4 and KK1 were kind gifts from Dr Y. Yamada (Nagasaki University, Nagasaki, Japan). Su9T-01 and S1T were kind gifts from Dr N. Arima (Kagoshima University, Kagoshima, Japan). ED was a kind gift from Dr M. Maeda (Kyoto University, Kyoto, Japan). AML cell lines UCSD/AML1, Kasumi-3, K051, NH and MOLM1 were obtained from Dr R. Taetle (VA Medical Center, Sepulveda, CA, USA), from Dr H. Asoh (Hiroshima University, Hiroshima, Japan), from Dr T. Nomura (Nippon Medical School, Tokyo, Japan), from Dr K. Suzukawa (University of Tsukuba, Ibaraki, Japan) and from the Fujisaki Cell Center, Hayashibara Biochemical Laboratories (Okayama, Japan), respectively, and OIH-1 and FKH-1 were obtained from Dr H. Hamaguchi (Musashino Red Cross Hospital). Pancreatic cancer cell lines KLM1, PK9 and PK45P, OSCC cell lines SAS, HO-1-U-1, Ca9-22, HSC2, HSC3, HSC4, HSQ89 and Sa3, cervical cancer cell line HeLa, human embryonic kidney cell line HEK293T and mouse embryonic fibroblast cell line NIH3T3 were obtained from RIKEN Bioresource Center (Tsukuba, Japan). Hepatic cancer cell lines HLF and HuH28 and breast cancer cell line SK-BR-3 were obtained from the Japanese Cancer Research Resources Bank (Tokyo, Japan). Hepatic cancer cell lines HepG2 and HuH7 were obtained from the Health Science Research Resources Bank (Osaka, Japan). Lung cancer cell lines A549, H322, H1395, H1437 and H1648 were obtained from the American Type Culture Collection (Rockville, MD, USA). Glioblastoma cell line A172 and neuroblastoma cell lines NH6 and NH12 were kind gifts from Dr Y. Hayashi (Gunma Children's Medical Center, Gunma, Japan). Prostate cancer cell line PC3 was a kind gift from Dr T. Ochiya (National Cancer Center Research Institute, Tokyo, Japan). Gastric cancer cell lines Mkb28, Mkb45, and KatoIII and ovarian cancer cell line SKOV3 were kind gifts from Dr H. Kataoka (University of Miyazaki, Miyazaki, Japan). IL2-dependent ATLL cell lines were maintained in RPMI 1640 medium (Wako) supplemented with 10% fetal bovine serum and 50 JRU per ml recombinant human IL2 (Takeda). HTLV-1-negative cell lines, cell lines transformed with HTLV-1 and IL2-independent ATLL cell lines were maintained in the same medium without IL2. The other cell lines were cultured in RPMI 1640 or Dulbecco's modified Eagle's medium (Wako) supplemented with 10% fetal bovine serum.

Patient samples. Blood samples were obtained with informed consent with approval by the Institutional Review Board of the Faculty of Medicine, University of Miyazaki. ATLL cells were collected from the patients at the time of hospital admission before the chemotherapy started. The diagnosis of ATLL was based on clinical features, hematological characteristics and the presence of anti-HTLV-1 antibodies in the sera. Monoclonal HTLV-1 provirus integration into the DNA of leukaemic cells was confirmed by Southern blot analysis in all cases. Peripheral blood mononuclear cells (PBMCs) obtained from healthy volunteers and patients with ATLL were purified by gradient centrifugation (Sigma-Aldrich). The procedure for the isolation of ATLL cells from PBMCs has been described elsewhere[54]. $CD4^+$ T cells were purified from PBMCs of healthy volunteers by using anti-CD4 magnetic beads (Miltenyi Biotec) according to the manufacturer's instructions.

Antibodies and reagents. A synthetic peptide (17-PGQTPEAAKTHSVET-31) of human NDRG2 conjugated to keyhole limpet haemocyanin was used for immunization to generate a rabbit polyclonal antibody against NDRG2 (ref. 55). Mouse monoclonal (M2) and rabbit polyclonal (F7425) antibodies against FLAG, and mouse monoclonal antibody (AC-15) against β-actin were purchased from Sigma-Aldrich. Rabbit monoclonal antibodies against PTEN (138G6), phospho-AKT (Ser473) (D9E), phospho-AKT (Thr308) (244F9), phospho-GSK3β (Ser9) (D85E12), GSK3β (27C10), and PP2A C Subunit (PP2Ac) (52F8), rabbit polyclonal antibodies against phospho-PTEN (Ser380/Thr382/383) (9554), non-phospho-PTEN (Ser380/Thr382/383) (9569), AKT (9272), FOXO1/4 (9462) and cleaved caspase-3 (9661), and mouse monoclonal antibodies against PTEN (26H9) and Myc-tag (9B11) were obtained from Cell Signaling Technology. Rabbit polyclonal antibodies against phospho-PTEN (Ser370) (07-889) and PI3K p85 (06-195) were obtained from Upstate/Millipore, rabbit polyclonal antibody against phospho-PTEN (Ser385) (44-1064G) was obtained from Biosource, mouse monoclonal antibody against SHIP1 (P1C1) and goat polyclonal antibody against NDRG2 (E20) were obtained from Santa Cruz Biotechnology, rabbit polyclonal antibody against GFP (598) was obtained from MBL, and rat monoclonal antibodies against mouse B220 (RA3-6B2), mouse CD4 (RM4-5) and mouse CD8 (53-6.7) and hamster monoclonal antibody against mouse CD3 (500A2) were obtained from BD Pharmingen. Mouse monoclonal antibody against TAX (MI73) was a kind gift from Dr M. Matsuoka (Kyoto University, Kyoto, Japan). Recombinant human PP2A core enzyme made up of polyhistidine-tagged (His_{8X}) human PP2Ac and FLAG-tagged human PR65/A co-expressed in baculovirus-infected High Five cell, OA and trichostatin A were obtained from Wako. Dimethyl 3,3′-dithiobispropionimidate (DTBP) was obtained from Thermo Fisher Scientific, and TBB was obtained from Calbiochem. CX-4945 was obtained from Selleckchem, and 5-aza-2′-deoxycytidine was obtained from Sigma-Aldrich.

Plasmid construction. Full-length complementary DNA (cDNA) of *NDRG2* was isolated by RT–PCR from total RNA of the MOLT4 cell line and subcloned into the p3XFLAG-myc-CMV-26 expression vector (Sigma-Aldrich) by standard cloning procedures (FLAG-NDRG2). The FLAG-tagged NDRG2 deletion constructs—NDRG2-deltaN (amino acids 26–357), NDRG2-deltaC (amino acids 1–304), NDRG2-NDR (amino acids 26–304), NDRG2-HD (amino acids 81–297) and NDRG2-Cterm (amino acids 259–357)—were generated by PCR using the NDRG2/pCMV26 as the template and subcloned into p3XFLAG-myc-CMV-26. The GFP-PTEN constructs—GFP-PTEN, GFP-PTEN-N (amino acids 1–185) and GFP-PTEN-C (amino acids 186–403)—were generated by PCR using the PTEN/pcDNA3 (a kind gift from Dr T. Kohno, National Cancer Center Research Institute, Tokyo, Japan) as the template and subcloned into pEGFP-C1 vector (Clontech). A full-length *PTEN* cDNA was amplified from the Su9T-01 cell line by PCR and subcloned into the p3XFLAG-myc-CMV-26. To generate substitution mutant PTEN expression vectors (PTEN-S370A, -S380A/T382A/T383A and -S385A), PCR-based mutagenesis were performed to introduce mutations in the PTEN coding sequence using mutagenic primers listed in Supplementary Table 8 and p3XFLAG-myc-CMV-26/PTEN plasmid as the template. All PCR-generated products were confirmed by nucleotide sequencing. The expression vector for constitutively active PI3K (pmycBD110)[56], which carries the p110-binding domain of p85α attached to the N-terminal region of p110, was kindly provided by Dr Y. Fukui (National Health Research Institutes, Taiwan). The myc-PP1c/pcDNA3, myc-PP2Ac/pcDNA3 and myc-PP5c/pcDNA3 constructs have been described elsewhere[57].

Bisulfite sequencing. A 200-ng DNA sample was denatured in 0.2 M NaOH followed by the addition of bisulfite solution (2.5 M sodium bisulfite, 10 mM hydroquinone and 240 mM NaOH). The mixture was then incubated at 55 °C for 16 h. DNA samples were desulfonated in 0.2 M NaOH and precipitated with ethanol. PCR was performed in a 20-μl volume containing 1 μl of bisulfite-treated DNA, 500 μM of dNTP and 500 nM of each primer for the *NDRG2* promoter region (nucleotides 20564110-20563790, GenBank accession no. NC_000014) (forward 5′-TTTTCGAGGGGTATAAGGAGAGTTTATTTT-3′ and reverse 5′-CCAAAAACTCTAACTCCTAAATAAACA-3′) (ref. 48), and 1 unit of Taq polymerase (Takara) under the following conditions: 98 °C for 30 s; 40 cycles of 98 °C for 10 s, 60 °C for 5 s and 72 °C for 30 s; and final extension at 72 °C for 3 min. PCR products were subcloned into the pTA2 vector (TOYOBO) and sequenced.

Real-time RT-PCR analysis. Total RNA was isolated from cells using TRIzol reagent (Invitrogen) and 1 μg of total RNA was reverse transcribed to obtain first-strand cDNA using an RNA-PCR kit (Takara) following the manufacturer's instructions. The resulting cDNA was used for real-time RT–PCR using a SYBR Green PCR Master Mix kit (Applied Biosystems). PCR was performed in a 25-μl volume containing 1 μl cDNA, 300 μM of each primer and 12.5 μl of 2 × PCR master mix under the following conditions: 95 °C for 10 min followed by 40 cycles of 95 °C for 15 s and 60 °C for 1 min. For NDRG2 primers, the cycling conditions were 95 °C for 10 min, 40 cycles of 95 °C for 15 s, 60 °C for 20 s and 72 °C for 40 s. The primers used were as follows: for *PTEN*, PTEN-F (5′-CAGCCATCATCAAAGAGATCG-3′) and PTEN-R (5′-TTGTTCCTGTATACGCCTTCAA-3′); for *NDRG2*, NDRG2-F (5′-CTGGAACAGCTACAACAACC-3′), and NDRG2-R (5′-TCAACAGGAGACCTCCATGG-3′); and for β-actin, ACTB-F (5′-GACAGGATGCAGAAGGAGATTACT-3′), and ACTB-R (5′-TGATCCACATCTGCTGGAAGGT-3′). The data were normalized to the amount of β-actin mRNA, and the values are represented as the mean ± s.d. of $2^{-\Delta\Delta Ct}$ in a duplicate assay.

Western blot analysis. Cell lysate samples were prepared in NP-40 lysis buffer (50 mM Tris–HCl, pH 8.0, 150 mM NaCl, 5 mM EDTA, 1% NP-40) supplemented with protease inhibitor cocktail (Sigma-Aldrich) and phosphatase inhibitors (PhosStop, Roche) or by direct lysis in boiling Laemmli SDS sample buffer (62.5 mM Tris–HCl, pH 6.8, 2% SDS, 25% glycerol, 5% β-mercaptoethanol and 0.01% bromophenol blue). Protein samples were electrophoresed on 10% SDS-polyacrylamide gel and transferred to polyvinylidine difluoride membranes (Immobilon-P, Millipore). The membranes were blocked in Tris-buffered saline (TBS)-Tween (0.1%) with either 5% bovine serum albumin (BSA) or 5% nonfat dried milk and were then incubated with each primary antibody diluted in TBS containing 0.1% Tween 20 supplemented with either 5% nonfat dried milk or 5% BSA or in the Can Get Signal buffer (TOYOBO). Bound antibody was detected by a Lumi-light Plus kit according to the manufacturer's instructions (Roche Diagnostics). Band intensities on blots were quantified using NIH Image J software. All primary antibodies were used at a dilution of 1:1,000, except anti-β-actin

(1:5,000) and anti-NDRG2 (E20, 1:250). Representative full-gel bots are provided in the Supplementary Fig. 22)

Immunoprecipitation assays. For detecting interaction between endogenous proteins, MOLT4 cells (1×10^7) and mouse frontal cortex tissue were solubilized with RIPA buffer (50 mM Tris–HCl, pH 7.8, 150 mM NaCl, 1% NP-40, 0.25% sodium deoxycholate and 1 mM EDTA) and NP-40 lysis buffer, respectively, supplemented with protease inhibitor cocktail (Sigma-Aldrich) and phosphatase inhibitors (PhosStop, Roche), and the lysates were then incubated with control rabbit immunoglobulin G or antibodies against NDRG2 (rabbit polyclonal, 1:500 or E20, 1:200) or PTEN (26H9, 1:100 or 138G6, 1:300), plus Protein G beads (Amersham Biosciences). After washing, the bound proteins were subjected to SDS-polyacrylamide gel electrophoresis (SDS-PAGE) and immunoblotting with antibodies against NDRG2 (rabbit polyclonal or E20) or PTEN (26H9 or 138G6). For overexpressed proteins, 293T cells were co-transfected with the indicated constructs using HilyMax (Dojindo) according to the manufacturer's instructions. After culturing for 48 h, the transfected cells were solubilized with RIPA buffer, and the lysates were then subjected to immunoprecipitation using FLAG M2 affinity gel (Sigma-Aldrich) or antibodies against GFP (1:200) or PTEN (138G6, 1:500), followed by immunoblotting with antibodies against either FLAG (F7425), GFP or PTEN (26H9). For chemical crosslinking, stable HUT102 or KK1 cell lines expressing FLAG-NDRG2 were washed twice with phosphate-buffered saline (PBS) and incubated with 2 mM DTBP in PBS at room temperature for 30 min. After washing twice with PBS, cells were lysed in TNT buffer (10 mM Tris–HCl, pH 7.5, 150 mM NaCl and 0.5% Triton X-100) supplemented with protease inhibitor cocktail (Sigma-Aldrich) and phosphatase inhibitors (Halt phosphatase inhibitor cocktail, Thermo Scientific), and the lysates were immunoprecipitated with control rabbit immunoglobulin G, antibody against PTEN (138G6, 1:500), or FLAG M2 affinity gel, followed by immunoblotting with antibodies against FLAG (F7425), PP2Ac, PTEN (138G6) or phospho-PTEN (Ser380/Thr382/Thr383).

Immunofluorescence staining. Cells were fixed with 4% paraformaldehyde for 10 min at room temperature, washed with TBS 0.1 M glycine, treated with 0.2% Triton X-100 and rewashed with TBS 0.1 M glycine. After blocking with 1% BSA in TBS, cells were incubated with primary antibodies against NDRG2 (E20, 1:100), FoxO1/4 (1:200), PTEN (138G6, 1:200) or FLAG (M2, 1:500) overnight at 4 °C. The cells were then washed three times with TBS containing 0.1% Tween 20 and incubated with Alexa Fluor-546 anti-mouse, Alexa Fluor-555 anti-rabbit, Alexa Fluor-488 anti-rabbit or Alexa Fluor-488 anti-goat secondary antibodies (Molecular Probes) at room temperature for 2 h. The coverslips were washed three times with TBS containing 0.1% Tween 20 and then mounted on glass slides using an antifade reagent (Invitrogen). Proteins were visualized using a confocal laser scanning microscope (Leica Microsystems). Nuclei were counterstained with 4′,6-diamidino-2-phenylindole (DAPI; Sigma-Aldrich).

RNAi treatment. DNA-based shRNA expression vector (RNAi-Ready pSIREN-RetroQ-ZsGreen vector, Clontech) and siRNA oligonucleotides were used in gene knockdown experiments. The shRNA target sequences were as follows: for human *NDRG2*, shNDRG2#1 (5′-GGTGGAGAGGGCATATGCA-3′) and shNDRG2#2 (5′-GCGAGTCTGGAACTCTTTCTT-3′); for mouse *NDRG2*, 5′-CCGTGAAGA ACAGTGGTAA-3′. A control shRNA vector targeting luciferase (shLuc) was purchased from Clontech. The PP2Acα siRNA (sc-43509) and control siRNA (6568) were purchased from Santa Cruz Biotechnology and Cell Signaling Technology, respectively. The transfections were performed using the Nucleofector V kit (Amaxa) following the company's protocol.

Cell proliferation assays. Cells were seeded onto 96-well microtiter plates at a density of 5×10^3 per well and cultured for the indicated time periods. Viable cells were counted by the methyl thiazolyl tetrazolium assay using a cell counting kit-8 (Dojindo). For stable transfectant cells, cells were seeded into 25 cm^2 flasks at a density of 1×10^5 ml^{-1}, and proliferation rates were assessed by counting the numbers of viable cells every 24 h using Trypan blue staining.

Dephosphorylation assay for synthetic peptides. The PTEN peptide 373-EPDHYRYSDTTDSDPENE-390 and phosphopeptides with pSer380 (EPDHYR-YpSDTTDSDPENE), pThr382 (EPDHYRYSDpTTDSDPENE), pThr383 (EPDHYRYSDTpTDSDPENE) and pSer380/pThr382/pThr383 (EPDHYR-YpSDpTpTDSDPENE) were obtained from TORAY Research Center (Tokyo, Japan). The release of inorganic phosphates from phosphopeptides was determined using a malachite green assay kit (BIOMOL Green reagent, BIOMOL). Cell extracts from the KK1-NDRG2 stable cell line, NIH3T3 cell line and 293T cell line transiently transfected with mock or Myc-tagged PP1c, PP2Ac or PP5c vectors using HilyMax were prepared by lysing cells in TNT buffer supplemented with protease inhibitor cocktail (Sigma-Aldrich). Endogenous PP2Ac and Myc-tagged PP1c, PP2Ac and PP5c were immunoprecipitated using antibodies against anti-PP2Ac (1:500) and anti-Myc (1:500), respectively. For inhibitor treatment, lysates of KK1-NDRG2 cells were incubated on ice for 30 min in the absence or presence of various concentrations of OA. The total cell lysates, immunoprecipitated samples or 0.5 units of recombinant PP2A were incubated with 100 μM PTEN peptide or phosphopeptides in 10 μl of phophatase assay buffer (20 mM HEPES pH 7.0, 1 mM $MnCl_2$, 8 mM $MgCl_2$, 1 mM dithiothreitol and 100 μg ml^{-1} BSA) at 30 °C for 60 min. The reactions were terminated by the addition of 40 μl of TE buffer (10 mM Tris–HCl, pH 8.0, 1 mM EDTA) and 100 μl of BIOMOL Green reagent, and absorbance at 620 nm was determined after incubation for 20 min at room temperature. The quantity of Pi released (nmoles) was calculated based on a standard curve determined for inorganic phosphate according to the manufacturer's recommendations. All assays were performed in duplicate.

PTEN dephosphorylation assay. The KK1-Mock stable cells were lysed in TNT buffer plus protease inhibitor cocktail (Sigma-Aldrich), and the cell lysates were immunoprecipitated with an antibody against PTEN (138G6, 1:500) and Protein G beads. Immunoprecipitates were washed three times with TNT buffer and twice with phosphatase assay buffer, resuspended in phosphatase assay buffer and incubated with 0.5 units of recombinant PP2A for 60 min at 30 °C. The reaction was stopped by adding SDS sample buffer, and the samples were separated by 10% SDS-PAGE, followed by western blotting with antibodies against PTEN (138G6) or phospho-PTEN (Ser370 or Ser380/Thr382/Thr383).

Generation of *NDRG2* knockout mice. *NDRG2*-deficient mice were generated in the Laboratory for Animal Resources and Genetic Engineering, RIKEN Center for Developmental Biology (accession. no. CDB0768K: http://www.cdb.riken.jp/arg/mutant%20mice%20list.html). For generating a targeting vector, genomic fragments for *NDRG2* were obtained from RP23-109J8 BAC clone (BACPAC Resources). A *lacZ*-pA-*neo*-pA cassette was inserted into exon 2 of the *NDRG2* gene to create the targeting construct. The linearized targeting vector was inserted into TT2 ES cells[58] by electroporation, and G418-resistant clones were screened for homologous recombination by PCR and Southern blot analysis using a 457-bp 5′ fragment as the probe. Targeted ES clones were microinjected into ICR eight-cell stage embryos and transferred into pseudopregnant ICR females (http://www.cdb.riken.jp/arg/Methods.html). The resulting chimeras were bred with C57BL/6 mice, and heterozygous offspring were identified by Southern blot analysis and by PCR using the following two primer pairs: WT allele, F1 (5′-CAAACACCCGA GACTGCCAA-3′)/R (5′-ATTAAACAATAAAGATGTCC-3′); targeted-allele, F2 (5′-GACAGGAGAGGATGAAGGTT-3′)/R. Heterozygous mice were backcrossed with C57BL/6 for two generations and mated in the same generation to obtain homozygous mutants. All animal experiments were approved by the Animal Experiment Review Board of the University of Miyazaki.

Histological analysis. All necropsies and histological examinations were performed on mice at the time of death. Tissues were fixed in 10% buffered formalin solution and embedded in paraffin blocks, and 2-μm-thick sections were prepared. Paraffinized sections were deparaffinized with xylene and rehydrated through a decreasing gradient of ethanol solutions. Slides were stained with hematoxylin and eosin (H&E), coverslipped with mounting medium, and viewed under a light microscope. The slides were scanned with a digital scanner (MIRAX; Carl Zeiss) and viewed with MIRAX software (Carl Zeiss). For immunohistochemistry, the tissue sections were deparaffinized and rehydrated. After microwave treatment for 20 min in citrate buffer pH 6.0 and cooling, endogenous peroxidase activity was blocked in 0.3% hydrogen peroxide in methanol for 30 min. After blocking in 5% skim milk in PBS for 30 min, sections were incubated with antibodies against CD3, CD4, CD8, B220, FLAG or cleaved caspase-3 for 60 min at 37 °C, washed three times with PBS and incubated with horseradish peroxidase-conjugated secondary antibodies for 30 min at 37 °C. The horseradish peroxidase activity was visualized with 3, 3′-diaminobenzidine containing hydrogen peroxide. All primary antibodies were used at 1:200 dilution, except anti-FLAG (1:500) and anti-cleaved caspase-3 (1:100).

Statistical analysis. Bars and markers in the figures represent the mean ± s.d. The two-tailed Student's *t*-test and Mann–Whitney *U*-test were used as appropriate. In the Kaplan–Meier survival analysis, the log-rank test was used for analysis. Fisher's exact analysis was used to determine differences in tumour incidence. Differences were considered significant when the *P* value was <0.05, as indicated in the text.

References

1. Takatsuki, K. *et al.* Clinical diversity in adult T-cell leukemia-lymphoma. *Cancer Res.* **45,** 4644s–4645s (1985).
2. Proietti, F. A., Carneiro-Proietti, A. B., Catalan-Soares, B. C. & Murphy, E. L. Global epidemiology of HTLV-I infection and associated diseases. *Oncogene* **24,** 6058–6068 (2005).
3. Yasunaga, J. & Matsuoka, M. Leukaemogenic mechanism of human T-cell leukaemia virus type I. *Rev. Med. Virol.* **17,** 301–311 (2007).
4. Fukuda, R. *et al.* Alteration of phosphatidylinositol 3-kinase cascade in the multilobulated nuclear formation of adult T cell leukemia/lymphoma (ATLL). *Proc. Natl Acad. Sci. USA* **102,** 15213–15218 (2005).

5. Ikezoe, T. *et al.* Longitudinal inhibition of PI3K/Akt/mTOR signaling by LY294002 and rapamycin induces growth arrest of adult T-cell leukemia cells. *Leuk. Res.* **31,** 673–682 (2007).
6. Li, J. *et al.* PTEN, a putative protein tyrosine phosphatase gene mutated in human brain, breast, and prostate cancer. *Science* **275,** 1943–1947 (1997).
7. Steck, P. A. *et al.* Identification of a candidate tumour suppressor gene, MMAC1, at chromosome 10q23.3 that is mutated in multiple advanced cancers. *Nat. Genet.* **15,** 356–362 (1997).
8. Hollander, M. C., Blumenthal, G. M. & Dennis, P. A. PTEN loss in the continuum of common cancers, rare syndromes and mouse models. *Nat. Rev. Cancer* **11,** 289–301 (2011).
9. Ali, I. U., Schriml, L. M. & Dean, M. Mutational spectra of PTEN/MMAC1 gene: a tumor suppressor with lipid phosphatase activity. *J. Natl Cancer Inst.* **91,** 1922–1932 (1999).
10. Cully, M., You, H., Levine, A. J. & Mak, T. W. Beyond PTEN mutations: the PI3K pathway as an integrator of multiple inputs during tumorigenesis. *Nat. Rev. Cancer* **6,** 184–192 (2006).
11. Song, M. S., Salmena, L. & Pandolfi, P. P. The functions and regulation of the PTEN tumour suppressor. *Nat. Rev. Mol. Cell Biol.* **13,** 283–296 (2012).
12. Trotman, L. C. *et al.* Ubiquitination regulates PTEN nuclear import and tumor suppression. *Cell* **128,** 141–156 (2007).
13. Wang, X. *et al.* NEDD4-1 is a proto-oncogenic ubiquitin ligase for PTEN. *Cell* **128,** 129–139 (2007).
14. Maddika, S. *et al.* WWP2 is an E3 ubiquitin ligase for PTEN. *Nat. Cell Biol.* **13,** 728–733 (2002).
15. Vazquez, F., Ramaswamy, S., Nakamura, N. & Sellers, W. R. Phosphorylation of the PTEN tail regulates protein stability and function. *Mol. Cell Biol.* **20,** 5010–5018 (2000).
16. Vazquez, F. *et al.* Tumor suppressor PTEN acts through dynamic interaction with the plasma membrane. *Proc. Natl Acad. Sci. USA* **103,** 3633–3638 (2006).
17. Odriozola, L., Singh, G., Hoang, T. & Chan, A. M. Regulation of PTEN activity by its carboxyl-terminal autoinhibitory domain. *J. Biol. Chem.* **282,** 23306–23315 (2007).
18. Rahdar, M. *et al.* A phosphorylation-dependent intramolecular interaction regulates the membrane association and activity of the tumor suppressor PTEN. *Proc. Natl Acad. Sci. USA* **106,** 480–485 (2009).
19. Silva, A. *et al.* PTEN posttranslational inactivation and hyperactivation of the PI3K/Akt pathway sustain primary T cell leukemia viability. *J. Clin. Invest.* **118,** 3762–3774 (2008).
20. Yang, Z. *et al.* Reduced expression of PTEN and increased PTEN phosphorylation at residue Ser380 in gastric cancer tissues: A novel mechanism of PTEN inactivation. *Clin. Res. Hepatol. Gastroenterol.* **37,** 72–79 (2013).
21. Torres, J. & Pulido, R. The tumor suppressor PTEN is phosphorylated by the protein kinase CK2 at its C terminus. Implications for PTEN stability to proteasome-mediated degradation. *J. Biol. Chem.* **276,** 993–998 (2001).
22. Hidaka, T. *et al.* Down-regulation of TCF8 is involved in the leukemogenesis of adult T-cell leukemia/lymphoma. *Blood* **112,** 383–393 (2008).
23. Popescu, N. C. Genetic alterations in cancer as a result of breakage at fragile sites. *Cancer Lett.* **192,** 1–17 (2003).
24. Yao, L., Zhang, J. & Liu, X. NDRG2: a Myc-repressed gene involved in cancer and cell stress. *Acta Biochim. Biophys. Sin. (Shanghai)* **40,** 625–635 (2008).
25. Fernandes, S., Iyer, S. & Kerr, W. G. Role of SHIP1 in cancer and mucosal inflammation. *Ann. NY Acad. Sci.* **1280,** 6–10 (2013).
26. Al-Khouri, A. M., Ma, Y., Togo, S. H., Williams, S. & Mustelin, T. Cooperative phosphorylation of the tumor suppressor phosphatase and tensin homologue (PTEN) by casein kinases and glycogen synthase kinase 3beta. *J. Biol. Chem.* **280,** 35195–35202 (2005).
27. Qu, X. *et al.* Characterization and expression of three novel differentiation-related genes belong to the human NDRG gene family. *Mol. Cell. Biochem.* **229,** 35–44 (2002).
28. Bialojan, C. & Takai, A. Inhibitory effect of a marine-sponge toxin, okadaic acid, on protein phosphatases, specificity and kinetics. *Biochem. J.* **256,** 283–290 (1988).
29. Hu, X. L. *et al.* Expression analysis of the NDRG2 gene in mouse embryonic and adult tissues. *Cell Tissue Res.* **325,** 67–76 (2006).
30. Lee, D. C. *et al.* Functional and clinical evidence for NDRG2 as a candidate suppressor of liver cancer metastasis. *Cancer Res.* **68,** 4210–4220 (2008).
31. Chang, X. *et al.* DNA methylation of NDRG2 in gastric cancer and its clinical significance. *Dig. Dis. Sci.* **58,** 715–723 (2013).
32. Furuta, H. *et al.* NDRG2 is a candidate tumor-suppressor for oral squamous-cell carcinoma. *Biochem. Biophys. Res. Commun.* **391,** 1785–1791 (2010).
33. Mavros, A. *et al.* Infrequent genetic alterations of the tumor suppressor gene PTEN/MMAC1 in squamous cell carcinoma of the oral cavity. *J. Oral Pathol. Med.* **31,** 270–276 (2002).
34. Kozaki, K. *et al.* PIK3CA mutation is an oncogenic aberration at advanced stages of oral squamous cell carcinoma. *Cancer Sci.* **97,** 1351–1358 (2006).
35. Leslie, N. R., Batty, I. H., Maccario, H., Davidson, L. & Downes, C. P. Understanding PTEN regulation: PIP2, polarity and protein stability. *Oncogene* **27,** 5464–5476 (2008).
36. Miller, S. J., Lou, D. Y., Seldin, D. C., Lane, W. S. & Neel, B. G. Direct identification of PTEN phosphorylation sites. *FEBS Lett.* **528,** 145–153 (2002).
37. Omori, N. *et al.* Enhanced phosphorylation of PTEN in rat brain after transient middle cerebral artery occlusion. *Brain. Res.* **954,** 317–322 (2002).
38. Ning, K. *et al.* A novel leptin signalling pathway via PTEN inhibition in hypothalamic cell lines and pancreatic beta-cells. *EMBO J.* **25,** 2377–2387 (2006).
39. Maccario, H., Perera, N. M., Davidson, L., Downes, C. P. & Leslie, N. R. PTEN is destabilized by phosphorylation on Thr366. *Biochem. J.* **405,** 439–444 (2007).
40. Wang, L. *et al.* NDRG2 is a new HIF-1 target gene necessary for hypoxia-induced apoptosis in A549 cells. *Cell. Physiol. Biochem.* **21,** 239–250 (2008).
41. Liu, J. *et al.* HIF-1 and NDRG2 contribute to hypoxia-induced radioresistance of cervical cancer Hela cells. *Exp. Cell Res.* **316,** 1985–1993 (2010).
42. Burchfield, J. G. *et al.* Akt mediates insulin-stimulated phosphorylation of Ndrg2: evidence for cross-talk with protein kinase C theta. *J. Biol. Chem.* **279,** 18623–18632 (2004).
43. Murray, J. T. *et al.* Exploitation of KESTREL to identify NDRG family members as physiological substrates for SGK1 and GSK3. *Biochem. J.* **384,** 477–488 (2004).
44. Eichhorn, P. J., Creyghton, M. P. & Bernards, R. Protein phosphatase 2A regulatory subunits and cancer. *Biochim. Biophys. Acta* **1795,** 1–15 (2009).
45. Rodgers, J. T., Vogel, R. O. & Puigserver, P. Clk2 and B56β mediate insulin-regulated assembly of the PP2A phosphatase holoenzyme complex on Akt. *Mol. Cell* **41,** 471–479 (2011).
46. Cheong, J. W. *et al.* Phosphatase and tensin homologue phosphorylation in the C-terminal regulatory domain is frequently observed in acute myeloid leukaemia and associated with poor clinical outcome. *Br. J. Haematol.* **122,** 454–456 (2003).
47. Kovács, K. A. *et al.* Phosphorylation of PTEN (phosphatase and tensin homologue deleted on chromosome ten) protein is enhanced in human fibromyomatous uteri. *J. Steroid Biochem. Mol. Biol* **103,** 196–199 (2007).
48. Lusis, E. A. *et al.* Integrative genomic analysis identifies NDRG2 as a candidate tumor suppressor gene frequently inactivated in clinically aggressive meningioma. *Cancer Res.* **265,** 7121–7126 (2005).
49. Tepel, M. *et al.* Frequent promoter hypermethylation and transcriptional downregulation of the NDRG2 gene at 14q11.2 in primary glioblastoma. *Int. J. Cancer* **123,** 2080–2086 (2008).
50. Piepoli, A. *et al.* Promoter methylation correlates with reduced NDRG2 expression in advanced colon tumour. *BMC Med. Genomics* **2,** doi:10.1186/1755-8794-2-11 (2009).
51. Barreau, O. *et al.* Identification of a CpG island methylator phenotype in adrenocortical carcinomas. *J Clin. Endocrinol. Metab.* **98,** E174–E184 (2013).
52. Kim, A. *et al.* Suppression of NF-kappaB activity by NDRG2 expression attenuates the invasive potential of highly malignant tumor cells. *Carcinogenesis* **30,** 927–936 (2009).
53. Park, Y. *et al.* SOCS1 induced by NDRG2 expression negatively regulates STAT3 activation in breast cancer cells. *Biochem. Biophys. Res. Commun.* **363,** 361–367 (2007).
54. Nakahata, S. *et al.* Clinical significance of CADM1/TSLC1/IgSF4 expression in adult T-cell leukemia/lymphoma. *Leukemia* **26,** 1238–1246 (2012).
55. Mitchelmore, C. *et al.* NDRG2: a novel Alzheimer's disease associated protein. *Neurobiol. Dis.* **16,** 48–58 (2004).
56. Kobayashi, M. *et al.* Expression of a constitutively active phosphatidylinositol 3-kinase induces process formation in rat PC12 cells. Use of Cre/loxP recombination system. *J. Biol. Chem.* **272,** 16089–16092 (1997).
57. Sugiyama, K. *et al.* Aurora-B associated protein phosphatases as negative regulators of kinase activation. *Oncogene* **21,** 3103–3111 (2002).
58. Yagi, T. *et al.* A novel ES cell line, TT2, with high germline-differentiating potency. *Anal. Biochem.* **214,** 70–76 (1993).

Acknowledgements

We thank Y. Motoyoshi, A. Nakatake and I. Morinaga for their technical assistance and N. Ishigami for secretarial assistance. We thank all of the members of the Division of Tumor and Cellular Biochemistry and HTLV-1/ATL Research Facility, University of Miyazaki for helpful discussions and comments. Also, we gratefully thank all of the researchers, who kindly provided us their important cell lines and materials. This work was supported by Grant-in-Aid for Scientific Research on Priority Areas (20012043) from the Ministry of Education, Culture, Sports, Science and Technology (MEXT) of Japan; Research fund from Miyazaki Prefecture Collaboration of Regional Entities for the Advancement of Technological Excellence (60G01-B7002022), Japan Science and Technology Agency (JST); Scientific Research (B) (21390098) (KM); and Young Scientists (B) (23701061 to SN and 23790372 to TI) of Japan Society for the Promotion of Science (JSPS).

Author contributions

S.N., T.I. and K.M. designed the research; S.N., T.I., M.H., N.Y. and Y.A. performed the experiments and analysed the results; P.M., T.T., K.O., N.M. and R.Y. performed the

histopathology; Y.S., K.N., T.T. and M.T. performed the SNP array analysis; T.A. and H.K. generated *NDRG2*-deficient mice; M.H. and K.N. performed the cDNA microarray analysis; K.N. and Y.K. performed the DNA methylation array analysis; K.S. provided patient samples; I.K. Y.A., T.T., A.H., and H.S. edited and commented on the manuscripts; S.N. and K.M. wrote the manuscript; K.M. supervised the project.

Additional information

Accession codes: The gene expression data have been deposited in the Gene Expression Omnibus database under accession code GSE43017.

Supplementary Information accompanies this paper at http://www.nature.com/naturecommunications

Competing financial interests: The authors declare no competing financial interests.

Reprints and permission information is available online at http://npg.nature.com/reprintsandpermissions/

How to cite this article: Nakahata, S. *et al.* Loss of NDRG2 expression activates PI3K-AKT signalling via PTEN phosphorylation in ATLL and other cancers. *Nat. Commun.* 5:3393 doi: 10.1038/ncomms4393 (2014).

Plants **2014**, *3*, 18-26; doi:10.3390/plants3010018

OPEN ACCESS

plants

ISSN 2223-7747

www.mdpi.com/journal/plants

Article

Identification of a Bioactive Compound against Adult T-cell Leukaemia from Bitter Gourd Seeds

Hisahiro Kai [1,2,*], Ena Akamatsu [2], Eri Torii [2], Hiroko Kodama [2,3], Chizuko Yukizaki [3], Isao Akagi [2,4], Hisatoshi Ino [5], Yoichi Sakakibara [6], Masahito Suiko [6], Ikuo Yamamoto [7], Akihiko Okayama [7], Kazuhiro Morishita [8], Hiroaki Kataoka [9] and Koji Matsuno [1]

1 Department of Pharmaceutical Health Sciences, School of Pharmaceutical Sciences, Kyushu University of Health and Welfare, 1714-1 Yoshino-machi, Nobeoka, Miyazaki 882-8508, Japan; E-Mail: kjmtsn@phoenix.ac.jp

2 Research Promotion Bureau for Collaboration of Regional Entities, Miyazaki Prefectural Industrial Support Foundation, 16500-2 Higashi-Kaminaka, Sadowara-cho, Miyazaki, Miyazaki 880-0303, Japan; E-Mails: rojopino@mac.com (E.A.); ushio16@fc.miyazaki-u.ac.jp (E.T.); hiroyoko33@hotmail.com (H.K.); akagi046@chem.agri.kagoshima-u.ac.jp (I.A.)

3 Miyazaki Prefectural Food Research and Development Center, 16500-2 Higashi-Kaminaka, Sadowara-cho, Miyazaki, Miyazaki 880-0303, Japan; E-Mail: yukizaki@iri.pref.miyazaki.jp

4 Department of Biochemical Science and Technology, Faculty of Agriculture, Kagoshima University, 1-21-24 Korimoto, Kagoshima, Kagoshima 890-0065, Japan

5 Miyazaki Agricultural Experiment Station, 5805 Shimonaka, Sadowara-cho, Miyazaki, Miyazaki 880-0212, Japan; E-Mail: ino-hisatoshi@pref.miyazaki.lg.jp

6 Department of Biochemistry and Applied Biosciences, Faculty of Agriculture, University of Miyazaki, 1-1 Gakuenkibanadai-nishi, Miyazaki, Miyazaki 889-2192, Japan; E-Mails: ysakaki@cc.miyazaki-u.ac.jp (Y.S.); msuiko@cc.miyazaki-u.ac.jp (M.S.)

7 Department of Rheumatology, Infectious Diseases and Laboratory Medicine, Faculty of Medicine, University of Miyazaki, 5200 Kihara Kiyotake, Miyazaki, Miyazaki 889-1692, Japan; E-Mails: yamamoto@fc.miyazaki-u.ac.jp (I.Y.); okayama@med.miyazaki-u.ac.jp (A.O.)

8 Division of Tumor and Cellular Biochemistry, Department of Medical Sciences, Faculty of Medicine, University of Miyazaki, 5200 Kihara Kiyotake, Miyazaki, Miyazaki 889-1692, Japan; E-Mail: kmorishi@fc.miyazaki-u.ac.jp

9 Section of Oncopathology and Regenerative Biology, Department of Pathology, Faculty of Medicine, University of Miyazaki, 5200 Kihara Kiyotake, Miyazaki, Miyazaki 889-1692, Japan; E-Mail: mejina@med.miyazaki-u.ac.jp

* Author to whom correspondence should be addressed; E-Mail: hkai@phoenix.ac.jp; Tel.: +81-982-23-5704; Fax: +81-982-23-5705.

Received: 31 October 2013; in revised form: 18 December 2013 / Accepted: 19 December 2013 / Published: 27 December 2013

Abstract: In our previous report, an 80% ethanol bitter gourd seed extract (BGSE) was found to suppress proliferation of adult T-cell leukemia (ATL) cell lines. The present study aimed to identify the bioactive compounds from BGSE specific against ATL. From the result of an HPLC-MS analysis, α-eleostearic acid (α-ESA) was present in BGSE at 0.68% ± 0.0022% (±SD, n = 5). In the cell proliferation test, α-ESA potently suppressed proliferation of two ATL cell lines (ED and Su9T01; IC_{50} = 8.9 and 29.3 μM, respectively) more than several other octadecanoic acids. However, α-ESA moderately inhibited phytohemagglutinin-activated human peripheral blood mononuclear cells (PBMC; IC_{50} = 31.0 μM). These results suggest that BGSE-derived α-ESA has potential as a functional food constituent because of its activity against ATL, particularly against ED cells. Moreover, α-ESA might be effective for the prevention of moderate adverse effects of ATL on normal T cells.

Keywords: adult T-cell leukemia; bitter gourd seed extract; α-eleostearic acid; phytohemagglutinin-activated human peripheral blood mononuclear cell

1. Introduction

Adult T-cell leukemia (ATL) occurs in a small population of human T-cell leukemia virus type I (HTLV-I) infected individuals. After transmission of HTLV-I, 2%–5% of carriers are likely to develop ATL after a long latency period (30–50 years) [1]. These patients have been frequently identified as being from a restricted area of tropical regions [2]. It is currently very difficult to effectively treat patients with ATL using existing therapeutic methods, and most clinical trials focus on chemotherapeutic treatment and allogeneic hematopoietic stem cell transplantation. Therefore, it is important to find appropriate therapeutic methods to prevent the development of ATL or to prolong survival after its occurrence.

In our previous report, we screened 52 agricultural plant samples for their ability to inhibit proliferation in seven kinds of ATL related cell lines to start structure of a study for finding potential drug candidates with the prevention of ATL. We found that an 80% ethanol bitter gourd (*Momordica charantia* L.) seed extract (BGSE) showed an inhibitory effect on the proliferation of ATL-related human leukemia cells [3].

Bitter gourd belongs to the Cucurbitaceae family and is cultivated worldwide as a vegetable crop. The fruit is not only used as a food, but also for its medicinal properties, such as anti-microbial, anti-diabetic, anti-HIV and anti-tumor activities, which were described in a recent review [4]. BGSE has also been reported to have anti-leukemic potential on human acute myelogenous leukemia cells (HL-60) [5]. However, HL-60 and ATL cell lines comprise different types of leukemia cells, and as there have been no reports about bioactive compounds from BGSE active against ATL, the effect of

BGSE on ATL cell proliferation requires elucidation. The aim of the present study was to identify bioactive compounds in BGSE exhibiting activity against ATL.

2. Results and Discussion

2.1. Identification of Active Compounds in BGSE

Figure 1a,b show the HPLC-DAD chromatogram (a) and HPLC-MS-total ion chromatogram (TIC) (b) of BGSE. As shown in Figure 1a, a major peak (peak 1: retention time (RT) = 8.570 min, λ = 270 nm) was detected for BGSE. The TIC showed several peaks (Figure 1b). Figure 1c shows the MS spectrum of the peak with the RT: 8.570 min. in Figure 1b, which shows a deprotonated molecular ion signal at *m/z* 277. This compound was estimated to be $C_{18}H_{29}O_2$ and was proposed to be α-ESA on the basis of reference data [6]. α-ESA was analyzed using the same method. Figure 1d–f shows the HPLC-DAD chromatogram (d), TIC (e) and MS spectrum (f) of α-ESA. α-ESA (50 μg/mL) showed a clear peak at 270 nm (Figure 1d, peak 2) and the same RT of peak 1 in Figure 1a (BGSE). The RT (8.570 min.) of the highest peak in TIC for α-ESA (Figure 1e, peak 2) was the same as peak 1 in Figure 1b. The MS spectrum of α-ESA (Figure 1f) showed the same result as the analysis of BGSE (Figure 1c). From these results, peak 1 in Figure 1 was determined to be α-ESA, and α-ESA is the main compound in BGSE.

We also attempted to quantitatively determine α-ESA in BGSE. Figure 2 shows the α-ESA calibration curve. The calibration curve showed good linearity (R^2 = 0.9977). α-ESA was contained in the concentration range of 34.0 and 34.2 μg/5 mg of freeze-dried bitter gourd seeds (0.68% ± 0.0022%, ±SD, n = 5). In our previous report, BGSE suppressed the proliferation of ATL cell lines [3]. The current study shows the presence of α-ESA in BGSE. Tsuzuki *et al.* reported that α-ESA accounted for about 60% of the total fatty acid composition of bitter gourd seed oil [7]. Therefore, α-ESA might have greatly contributed to suppressing the proliferation of ATL cell lines.

2.2. The Inhibitory Effects of Octadecanoic Acid Analogs on ATL Cell Lines

Of the octadecanoic acids, conjugated linoleic acids (CLA), which includes α-ESA, has been acknowledged to have numerous biological activities, such as anti-obesity, anti-diabetes, anti-cancer, anti-arthritis, anti-asthma, and anti-cardiovascular disease effects [8]. However, no study has yet reported the anti-leukemic effects of α-ESA on ATL cell lines. We examined the inhibitory effects of related compounds, seven octadecanoic acid groups, on the proliferation of two types of ATL cell lines (ED and Su9T01). As shown in Table 1, α-ESA (C18:3, n-5), γ-linolenic acid (C18:3, n-6), and α-linolenic acid (C18:3, n-3), which belong to the triunsaturated fatty acid group, substantially inhibited ED cell growth (IC_{50} values of 8.9, 61.3 and 129.9 μM, respectively) and Su9T01 cell growth (IC_{50} values of 29.3, 174.3 and 167.4 μM, respectively). Linoleic acid (C18:2, n-6), which belongs to the diunsaturated fatty acid group, inhibited ED and Su9T01 cell growth (IC_{50} values of 100.7 and 180.1 μM, respectively). In ED cells, these compounds exhibited higher activity than EGCG, which was used as the positive control [9] (IC_{50} = 152.7 μM). On the other hand, in Su9T01 cells, only α-ESA exhibited higher inhibitory activity than EGCG (IC_{50} = 166.0 μM). We cannot calculate the exactly IC_{50} values of monounsaturated fatty acid group (oleic acid (C18:1, n-9) and elaidic acid

(C18:1, n-9)) and saturated fatty acid (stearic acid (C18:0)) in both cell lines. This assay was employed to compare the effects of octadecanoic acids on ED and Su9T01 cell growth; α-ESA showed the highest inhibitory activity. IC_{50} values decreased roughly in proportion to the number of double bonds; therefore, the number of double bonds was an important determinant of anti-proliferation activity. Indeed, the triunsaturated fatty acid group was more potent than EGCG.

Figure 1. HPLC-DAD and MS chromatograms of BGSE and α-ESA. (**a**,**d**) HPLC-DAD chromatograms (270 nm) of BGSE (**a**) and α-ESA (**d**). (**b**,**e**) Total ion chromatograms (TIC) of BGSE (**b**) and α-ESA (**e**). (**c**) MS spectrum (negative-ion spectra) of peak 1 of BGSE in Figure 1b. (**f**) MS spectrum (negative-ion spectra) of peak 2 of α-ESA in Figure 1e.

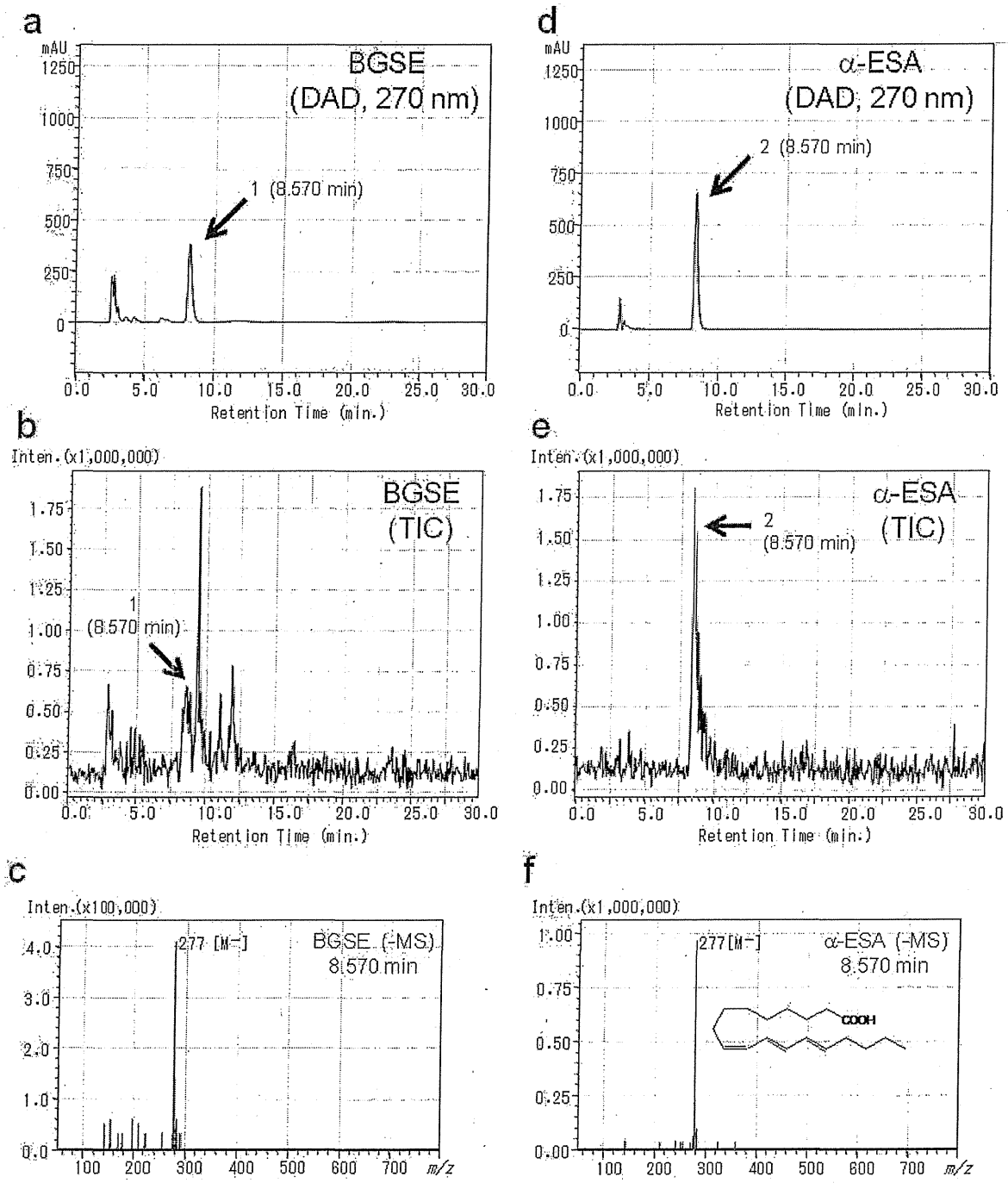

Figure 2. Calibration curve of α-ESA.

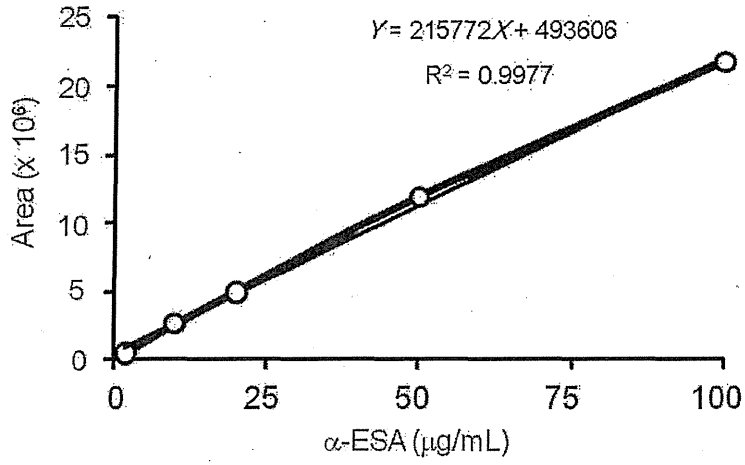

Table 1. Relationship between octadecanoic acid structure and inhibition of adult T-cell leukemia (ATL) cell line proliferation.

Compounds		IC_{50} (μM)	
		ED	**Su9T01**
α-ESA	(C18:3, n-5)	8.9	29.3
γ-linolenic acid	(C18:3, n-6)	61.3	174.3
α-linolenic acid	(C18:3, n-3)	129.9	167.4
linoleic acid	(C18:2, n-6)	100.7	180.1
oleic acid	(C18:1, n-9)	500.0–166.7	500.0–166.7
elaidic acid	(C18:1, n-9)	>500.0	>500.0
stearic acid	(C18:0)	500.0–166.7	>500.0
EGCG	(Positive Control)	152.7	166.0

ATL cells (ED and Su9T01) were incubated for 72 h in RPMI-1640 medium containing each compound. Viable cells were detected using a WST-8 assay kit. The concentration at which cell proliferation is inhibited by 50% compared to untreated control is expressed as IC_{50}.

2.3. The Effect of α-ESA on ATL Cell Line and Phytohemagglutinin-Activated Human Peripheral Blood Mononuclear Cell (PBMC) Proliferation

As shown in Figure 3, we compared the suppressive effect of α-ESA on ED, Su9T01 cells and PBMCs. PBMCs are commonly used as the healthy/normal cell model in comparison to cancer cell lines. Significant differences were observed between ED cells and PBMCs treated at 6, 19 and 56 μM α-ESA ($p < 0.05$). Su9T01 cells and PBMCs treated with between 1 and 500 μM α-ESA were not significantly different. These results confirmed that the α-ESA strongly and selectively inhibited ED cells and moderately inhibited PBMCs, which are healthy normal T cells. α-ESA at 166 and 500 μM significantly decreased proliferation of all cell types. α-ESA showed inhibitory effects on ED, Su9T01 cells and PBMCs (IC_{50} of 8.9, 29.3 and 31.0 μM, respectively).

Figure 3. Effect of α-ESA on ATL cell and PBMC proliferation.

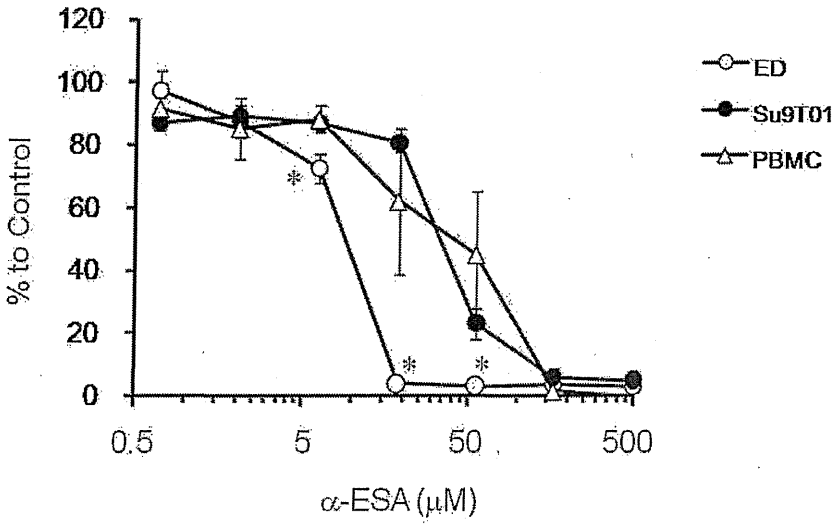

A comparison of the dose-dependent effects of α-ESA on ED, Su9T01 cells and PBMCs. Each mark represents the mean ± SD of three independent tests (Student's *t*-test). Significantly different between ED cells and PBMCs: $p < 0.05$ (*).

Tsuzuki *et al.* and Kobori *et al.* reported that bitter gourd seed oil and its constituent α-ESA had anti-leukemic potential in HL-60 cells [5,10]. While HL-60 and ATL (ED and Su9T01) are leukemia cell lines, they differ in origin and whether they are a result of viral infection. The antiproliferative properties of unsaturated fatty acids are well known. For example, Wendel *et al.* reported that the unsaturated fatty acids (mainly omega-3 fatty acids and derivatives) like conjugated eicosapentaenoic acid as important nutritional adjuvant therapeutics in the management of various human cancer diseases and the impact of nutritional omega-3 fatty acids on cancer prevention [11]. α-ESA also may have similar potential with nutritional function for cancer prevention. The present study is the first to show the inhibitory effects of α-ESA on ATL cells *in vitro*. Specifically, α-ESA showed an inhibitory effect in the rank order: ED cells > Su9T01 cells ≥ PBMCs. Sasaki *et al.* reported that tumor suppressor in lung cancer 1 (*TSLC1*) gene expression was different between ED and Su9T01 cells [12,13]. Therefore, using gene expression analysis, future studies should investigate the regulatory mechanism of *TSLC1* and its DNA methylation, as well as the possible role of α-ESA in the inhibition of ED and Su9T01 proliferation and *TSLC1* expression.

3. Experimental

3.1. Chemicals

α-Eleostearic acid (α-ESA) was obtained from Larodan Fine Chemicals AB, Malmö, Sweden and Cayman Chemical, Ann Arbor, MI, USA. γ-Linolenic acid, linoleic acid, α-linolenic acid, and elaidic acid were purchased from Cayman Chemical. Stearic acid and oleic acid were purchased from Wako, Osaka, Japan. Epigallocatechin-3-gallate (EGCG) was purchased from Nagara Science Co., Gifu, Japan. Ficoll was purchased from GE Healthcare, Uppsala, Sweden. Phytohemagglutinin (M Form) was purchased from Invitrogen, Carlsbad, CA, USA. IL-2 was purchased from R&D Systems,

Minneapolis, MN, USA. A 2-(2-methoxy-4-nitrophenyl)-3-(4-nitrophenyl)-5-(2,4-disulfophenyl)-2*H*-tetrazolium monosodium salt (WST-8) assay kit was purchased from Dojindo, Kumamoto, Japan.

3.2. Identification of Compounds in BGSE

The freeze-dried powder of bitter gourd seeds (5 mg) was extracted with 80% EtOH (0.5 mL) by vortexing for 30 s, followed by centrifugation at 1,500 rpm for 3 min. The supernatant was used for high performance liquid chromatography-diode array detector (HPLC-DAD) and mass spectrometry (MS) analysis. The α-ESA HPLC analysis method was a modification of the methods of Amakura *et al.* and Řezanka *et al.* [6,14]. The HPLC-DAD and MS analysis consisted of a Shimadzu HPLC System (LC-20A Prominence, Shimadzu, Kyoto, Japan) coupled to a SPD-20A (DAD; Shimadzu, Kyoto, Japan) and an LC/MS-ion trap-time of flight (LC/MS-IT-TOF, Shimadzu, Kyoto, Japan) fitted with an atmospheric pressure chemical ionization (APCI) source. HPLC separation was performed on a reverse-phase column (Atlantis T3, 2.1 mm I.D. ϕ100 mm, 3 μm; Waters, Milford, MA, USA). The column was maintained at 40 °C. The mobile phase consisted of eluent A (0.1% acetic acid and MeOH)/eluent B (0.1% acetic acid and 10% MeOH aq.) = 90:10 at a flow rate of 0.10 mL/min. The injection volume was 10 μL. APCI conditions were recorded from m/z = 50 to 400 in negative ion mode. The other MS conditions were as follows: nebulizer N_2 gas, 2.5 L/min; APCI interface temperature, 400.0 °C; curved desolvation line (CDL) temperature, 250.0 °C; heat block temperature, 200.0 °C; detector voltage, 1.80 kV.

3.3. α-ESA Calibration Curve

The α-ESA standard was dissolved in 80% ethanol and serial dilutions were analyzed by HPLC-DAD. α-ESA content was calculated using the following linear equation based on the calibration curve: $Y = 215772X + 493606$, $R^2 = 0.9977$. Y is the area detected by DAD (270 nm), and X is the α-ESA content in μg/mL.

3.4. ATL Cell Proliferation Assay

We used two ATL cell lines (ED and Su9T01) that are highly sensitive to inhibition of cell proliferation, as determined in our previous study [3]. ED cells were kindly provided by Dr. M. Maeda (Kyoto University, Kyoto, Japan) and Su9T01 cells were kindly provided by Dr. N. Arima (Kagoshima University, Kagoshima, Japan). The test compounds were dissolved in dimethyl sulfoxide and subjected to assay screening. The method of ATL assay is described in a previous report [3]. IC_{50} calculation was some curve fitted onto the determined proliferation inhibition points.

3.5. Isolation and Culture of PBMCs

The method of isolation and culture of PBMCs is as follows. Heparinised blood (5 mL) was diluted by adding 5 mL of PBS. The diluted blood samples were divided into four equal parts, loaded on 4 mL of Ficoll and centrifuged at 400 × g for 30 min. The PBMC layer was located within the interphase between the Ficoll and plasma. The Ficoll contained the erythrocytes and most of the granulocytes. The plasma was removed using a pipette until ~5 mL above the PBMC interphase. The cells were

washed three times with PBS (centrifuged at 200 × *g* for 15 min) and resuspended in RPMI 1640 medium supplemented with 10% foetal bovine serum containing 100 U/mL penicillin G, 100 μg/mL streptomycin, 2 ng/mL IL-2 and 128-fold dilution of phytohemagglutinin to a final cell density of 1×10^6 cells/mL. The PBMC proliferation assay was conducted using the same method as for the ATL proliferation assay [3].

3.6. Statistics

Each experiment was conducted at least three times. All data are expressed as the mean ± standard deviation (SD) of three independent experiments. Statistically significant differences were calculated by Student's *t*-test.

4. Conclusions

α-ESA was shown to be the main bioactive compound in BGSE, and contributes to the inhibition of ED cell differentiation and proliferation without damaging normal cells, leading to the disruption of ATL pathogenesis.

Acknowledgments

We thank Michiyuki Maeda (Kyoto University) and Naomichi Arima (Kagoshima University) for supplying the cell lines. We also thank Yuuki Maeda and Naomi Makisumi for their excellent technical assistance. This work was supported by a Grant-in-Aid from the Collaboration of Regional Entities for the Advancement of Technological Excellence (CREATE) from the Japanese Science and Technology Agency.

Conflicts of Interest

The authors declare no conflict of interest.

References

1. Arisawa, K.; Soda, M.; Endo, S.; Kurokawa, K.; Katamine, S.; Shimokawa, I.; Koba, T.; Takahashi, T.; Saito, H.; Doi, H.; *et al.* Evaluation of adult T-cell leukemia/lymphoma incidence and its impact on non-Hodgkin lymphoma incidence in southwestern Japan. *Int. J. Cancer* **2000**, *85*, 319–324.
2. Proietti, F.A.; Carneiro-Proietti, A.B.; Catalan-Soares, B.C.; Murphy, E.L. Global epidemiology of HTLV-I infection and associated diseases. *Oncogene* **2005**, *24*, 6058–6068.
3. Kai, H.; Akamatsu, E.; Torii, E.; Kodama, H.; Yukizaki, C.; Sakakibara, Y.; Suiko, M.; Morishita, K.; Kataoka, H.; Matsuno, K. Inhibition of proliferation by agricultural plant extracts in seven human adult T-cell leukaemia (ATL)-related cell lines. *J. Nat. Med.* **2011**, *65*, 651–655.
4. Fang, E.F.; Ng, T.B. Bitter gourd (*Momordica charantia*) is a cornucopia of health: A review of its credited antidiabetic, anti-HIV, and antitumor properties. *Curr. Mol. Med.* **2011**, *11*, 417–436.

5. Soundararajan, R.; Prabha, P.; Rai, U.; Dixit, A. Antileukemic Potential of *Momordica charantia* Seed Extracts on Human Myeloid Leukemic HL60 Cells. *J. Evid.-Based Complement. Alternat. Med.* **2012**, doi:10.1155/2012/732404.
6. Amakura, Y.; Kondo, K.; Akiyama, H.; Ito, H.; Hatano, T.; Yoshida, T.; Maitani, T. Characteristic long-chain fatty acid of *Pleurocybella porrigens*. *Shokuhin Eiseigaku Zasshi* **2006**, *47*, 178–181.
7. Tsuzuki, T.; Tokuyama, Y.; Igarashi, M.; Miyazawa, T. Tumor growth suppression by alpha-eleostearic acid, a linolenic acid isomer with a conjugated triene system, via lipid peroxidation. *Carcinogenesis* **2004**, *25*, 1417–1425.
8. Ruiz, R.A.; Reglero, G.; Ibañez, E. Recent trends in the advanced analysis of bioactive fatty acids. *J. Pharm. Biomed. Anal.* **2012**, *51*, 305–326.
9. Li, H.C.; Yashiki, S.; Sonoda, J.; Lou, H.; Ghosh, S.K.; Byrnes, J.J.; Lema, C.; Fujiyoshi, T.; Karasuyama, M.; Sonoda, S. Green tea polyphenols induce apotosis *in vitro* in peripheral blood T lymphocytes of adult T-cell leukemia patients. *Jpn. J. Cancer Res.* **2000**, *91*, 34–40.
10. Kobori, M.; Ohnishi-Kameyama, M.; Akimoto, Y.; Yukizaki, C.; Yoshida, M. α-eleostearic acid and its dihydroxy derivative are major apoptosis-inducing components of bitter gourd. *J. Agric. Food Chem.* **2008**, *56*, 10515–10520.
11. Wendel, M.; Heller, A.R. Anticancer actions of omega-3 fatty acids—Current state and future perspectives. *Anticancer Agents Med. Chem.* **2009**, *9*, 457–470.
12. Sasaki, H.; Nishikata, I.; Shiraga, T.; Akamatsu, E.; Fukami, T.; Hidaka, T.; Kubuki, Y.; Okayama, A.; Hamada, K.; Okabe, H.; *et al.* Overexpression of a cell adhesion molecule, TSLC1, as a possible molecular marker for acute-type adult T-cell leukemia. *Blood* **2005**, *105*, 1204–1213.
13. Watanabe, M.; Nakahata, S.; Hamasaki, M.; Saito, Y.; Kawano, Y.; Hidaka, T.; Yamashita, K.; Umeki, K.; Taki, T.; Taniwaki, M.; *et al.* Downregulation of CDKN1A in adult T-cell leukemia/lymphoma despite overexpression of CDKN1A in human T-lymphotropic virus 1-infected cell lines. *J. Virol.* **2010**, *84*, 6966–6977.
14. Řezanka, T.; Votruba, J. Analysis of Fatty Acids by APCI-MS. In *Modern Methods for Lipid Analysis by Liquid Chromatography: Mass Spectrometry and Related Techniques*; William, C.B., Ed.; AOCS Press: Urbana, IL, USA, 2005; pp. 242–275.

Biochemical and Biophysical Research Communications 441 (2013) 102–107

Contents lists available at ScienceDirect

Biochemical and Biophysical Research Communications

journal homepage: www.elsevier.com/locate/ybbrc

Suppressed expression of *NDRG2* correlates with poor prognosis in pancreatic cancer

Akihiro Yamamura [a,b], Koh Miura [a], Hideaki Karasawa [a], Kazuhiro Morishita [c], Keiko Abe [b], Yasuhiko Mizuguchi [b], Yuriko Saiki [b], Shinichi Fukushige [b], Naoyuki Kaneko [a], Tomohiko Sase [a], Hiroki Nagase [d], Makoto Sunamura [a,b,e], Fuyuhiko Motoi [a], Shinichi Egawa [a], Chikashi Shibata [a], Michiaki Unno [a], Iwao Sasaki [a], Akira Horii [b,*]

[a] Department of Surgery, Tohoku University, Graduate School of Medicine, Sendai, Japan
[b] Department of Pathology, Tohoku University, Graduate School of Medicine, Sendai, Japan
[c] Department of Medical Sciences, Faculty of Medicine, University of Miyazaki, Miyazaki, Japan
[d] Department of Advanced Medical Science, Nihon University School of Medicine, Tokyo, Japan
[e] Department of Digestive Tract Surgery and Transplantation Surgery, Tokyo Medical University, Hachioji Medical Center, Tokyo, Japan

ARTICLE INFO

Article history:
Received 2 October 2013
Available online 14 October 2013

Keywords:
NDRG2
Epigenetic silencing
Hypermethylation
Pancreatic cancer
Prognostic factor

ABSTRACT

Pancreatic cancer is a highly lethal disease with a poor prognosis; the molecular mechanisms of the development of this disease have not yet been fully elucidated. N-myc downstream regulated gene 2 (*NDRG2*), one of the candidate tumor suppressor genes, is frequently downregulated in pancreatic cancer, but there has been little information regarding its expression in surgically resected pancreatic cancer specimens. We investigated an association between NDRG2 expression and prognosis in 69 primary resected pancreatic cancer specimens by immunohistochemistry and observed a significant association between poor prognosis and NDRG2-negative staining ($P = 0.038$). Treatment with trichostatin A, a histone deacetylase inhibitor, predominantly up-regulated *NDRG2* expression in the *NDRG2* low-expressing cell lines (PANC-1, PCI-35, PK-45P, and AsPC-1). In contrast, no increased *NDRG2* expression was observed after treatment with 5-aza-2′ deoxycytidine, a DNA demethylating agent, and no hypermethylation was detected in either pancreatic cancer cell lines or surgically resected specimens by methylation specific PCR. Our present results suggest that (1) *NDRG2* is functioning as one of the candidate tumor-suppressor genes in pancreatic carcinogenesis, (2) epigenetic mechanisms such as histone modifications play an essential role in *NDRG2* silencing, and (3) the expression of NDRG2 is an independent prognostic factor in pancreatic cancer.

1. Introduction

Pancreatic cancer is a highly lethal disease; few patients are diagnosed at a state early enough for curative treatments. It is the fourth most common cause of cancer death worldwide [1], and the long-term prognosis remain poor with a 5-year survival rate of less than 5% after the initial diagnosis [2]. One of the major hallmarks of pancreatic cancer is its extensive local tumor invasion and early systemic dissemination. The molecular basis for these characteristics of pancreatic cancer is incompletely understood.

N-Myc downstream regulated gene 2 (*NDRG2*) is a member of *NDRG* gene family that is highly expressed in many normal tissue types, including brain, spinal cord, skeletal muscle, heart, and salivary gland [3–5]. *NDRG* gene family members share 53–65% homologous amino acid sequences with each other. Each member has a distinct tissue specificity of expression and may be intimately involved in cell proliferation, differentiation, development, and stress responses [6].

NDRG2 has been reported to be a candidate tumor suppressor gene, and its expression is downregulated in a number of primary tumors developed in organs of brain and meninges [4,7,8], liver [9,10], pancreas [10], esophagus [11], stomach [12], colorectum [6,13,14], kidney [6], thyroid [15], oral cavity [16], prostate [17], gallbladder [18], blood [19], and lung [20]. *NDRG2* is reported to

Abbreviations: *NDRG2*, N-myc downstream regulated gene 2; 5-aza-dC, 5-aza-2′ deoxycytidine; TSA, trichostatin A; qRT-PCR, quantitative reverse transcription polymerase chain reaction; cDNA, complementary DNA; AU, arbitrary unit; *B2M*, β2-microglobulin; MSP, methylation-specific PCR; HDAC, histone deacetylase.

* Corresponding author. Address: Department of Pathology, Tohoku University, Graduate School of Medicine, 2-1 Seiryo-machi, Aoba-ku, Sendai 980-8575, Japan. Fax: +81 22 717 8047.
E-mail address: horii@med.tohoku.ac.jp (A. Horii).

0006-291X/$ - see front matter © 2013 Elsevier Inc. All rights reserved.
http://dx.doi.org/10.1016/j.bbrc.2013.10.010

suppress proliferation and metastasis, and expressional inactivation of *NDRG2* may play an important role in carcinogenesis [4,9,11,12,21,22]. Several possible mechanisms, including promoter hypermethylation [7–9,13,16,23] and/or repression by MYC [4,11,14,15,24], are responsible for such expressional suppression. However, the precise mechanisms that lead to inactivation of *NDRG2* remain largely unknown, and role of *NDRG2* in human carcinogenesis is not yet well understood.

In the present study using immunohistochemistry, we found a significant association between poor prognosis and suppressed expression of NDRG2 in primary pancreatic cancer. Furthermore, *NDRG2* gene expression was up-regulated by histone deacetylase inhibitor in pancreatic cancer. It is notable that this histone modification has never previously been demonstrated in suppression of *NDRG2* expression in human cancer. These findings suggest that *NDRG2* is likely to be a novel prognostic marker and important indicator for a possible role of *NDRG2* in pancreatic cancer.

2. Materials and methods

2.1. Tissue specimens

A total of 69 pancreatic cancer tissues obtained from surgically resected specimens at Tohoku University Hospital (Sendai, Miyagi, Japan) during the period from 1997 to 2006 were analyzed. The clinical and histopathological characteristics of the pancreatic cancer patients are summarized in Table 1. Staging followed the TNM Classification of Malignant Tumor (6th edition) [25]. None of the patients had received any preoperative adjuvant therapy. The resected tissue specimens from these patients were fixed in 10% formalin and embedded in paraffin. Written informed consent was obtained from all patients. The study was approved by the Ethics Committee of Tohoku University School of Medicine.

Table 1
Relationship between NDRG2 expression and clinicopathological features of pancreatic cancer patients.

	NDRG2 expression		*P*-value
	Positive $n = 18$	Negative $n = 51$	
Gender			
Male	14	32	0.24
Female	4	19	
Age (mean, years)	61.2	64.0	0.25
Tumor size[a] (mm)	38.3	42.3	0.45
UICC Stage			
I	2	2	0.70
II	6	21	
III	6	16	
IV	4	12	
Differentiation			
Wel	2	1	0.14
Mod	15	41	
Por	1	9	
Lymph node metastasis			
N0	6	18	0.88
N1	12	33	
Lymphatic invasion			
Absent	3	5	0.61
Present	15	46	
Venous invasion			
Absent	0	4	0.22
Present	18	47	
Intrapancreatic neural invasion			
Absent	1	2	0.77
Present	17	49	

[a] Average longitudinal diameter.

2.2. Tissue array analysis and immunohistochemistry

A tissue array consisting of 69 paired pancreatic cancer and their corresponding normal tissues was constructed using TISSUE MICROPROCESSOR (AZUMAYA, Tokyo, Japan). Each paraffin-embedded block was cored out at a diameter of 3 mm, and the cored columns were re-embedded in paraffin. For further analyses, 4 μm slide sections were prepared. The immunohistochemical assay was done by the avidin–biotin–peroxidase method described previously [26]. Rabbit polyclonal anti-NDRG2 (1:3000, Atlas Antibodies AB, Stockholm, Sweden) and anti-rabbit (1:1000, Amersham Biosciences, Little Chalfont, UK) secondary antibodies were used. Immunoreactivity was evaluated by two pathologists. NDRG2 immmunoreactivity was detected in both the cytoplasm and the plasma membrane. Normal epithelial cells showed expression of NDRG2 in all specimens. NDRG2 immunoreactivity was defined by comparison the signal intensities of normal and cancerous tissues; strong, moderate, and weak designations denote signals with cancerous tissue that were stronger, similar, or weaker than the normal tissues, respectively. When no NDRG2 signal was detected, we defined the tumor as negative.

2.3. Cell lines analyzed in this study

Nine human pancreatic cancer cell lines (PANC-1, PCI-35, PK-45P, AsPC-1, BxPC-3, PK-1, MIAPaCa-2, PK8 and PK9) and two colorectal cancer cell lines (Clone A and LS174T) were used. These cell lines were also used in our previous studies and were maintained as described [27,28].

2.4. RNA and DNA extraction

Total RNAs from cultured cells were extracted using RNeasy Mini Kit (Qiagen, Valencia, CA), and their concentrations were determined using a NanoDrop ND-1000 Spectrophotometer (NanoDrop Technologies, Wilmington, DE). Genomic DNAs from cultured cells were extracted using DNeasy Blood & Tissue Kits (Qiagen) according to the manufacturer's instructions, and their concentrations were measured with a NanoDrop ND-1000 Spectrophotometer. All the processes were carried out according to the manufacturers' instructions.

2.5. Quantitative reverse transcription PCR (qRT-PCR)

Each aliquot of 2 μg total RNA was reverse transcribed to synthesize cDNA using a High Capacity cDNA Reverse Transcription Kit (Applied Biosystems, Foster City, CA) according to the manufacturer's instructions. qRT-PCR analyses were performed using an ABI PRISM 7000 Sequence Detection System (Applied Biosystems) following the manufacturer's instructions. Expression of β2-microglobulin (*B2M*) was used as the internal control [29]. The nucleotide sequences for primers, probes, and PCR conditions are listed in Table 2. Amplifications were carried out in the 15 μl reaction mixtures according to methods described previously [30]. The expression ratios of *NDRG2*/*B2M* were calculated and used for characterization. Each experiment was performed in triplicate.

2.6. 5-Aza-2′-deoxycytidine (5-aza-dC) and trichostatin A (TSA) treatment

Cells were seeded at a density of 2×10^6 cells per 100 mm dish and were maintained for 72 h while replacing the culture medium containing 1 μM 5-aza-dC (Sigma, St. Louis, MO) every 24 h. Subse-

Table 2
Nucleotide sequences of the primers and probes.

	Forward primer (5′–3′)	Reverse primer (5′–3′)	Probe (5′–3′)	Annealing temperature (°C)	PCR cycles	Product size (bp)
qRT-PCR						
NDRG2	GAAGATGCAGTGGTGGAATG	TCAGCTTGCCTGGCTGAGT	TTCCTCAAGATGGCTGACTCCGG	60	30	109
B2M[a]	TTTCAGCAAGGACTGGTCTTT	CCAAATGCGGCATCTTCAAAC	CTGAAAAAGATGAGTATGCCTGCCGTGTG	60	30	171
MSP						
Methylation specific primer	GTTTGCGGGAAGTTCGAGTC	CCGCCGACCCGACTAACG		70	35	134
Unmethylation specific primer	GTGGGTTTGTGGGAAGTTTGAGTTG	CCACCCACCAACCCAACTAACA		70	30	142

[a] Nucleotide sequences for *B2M* primers and probe were previously reported by Ogawa et al. [29].

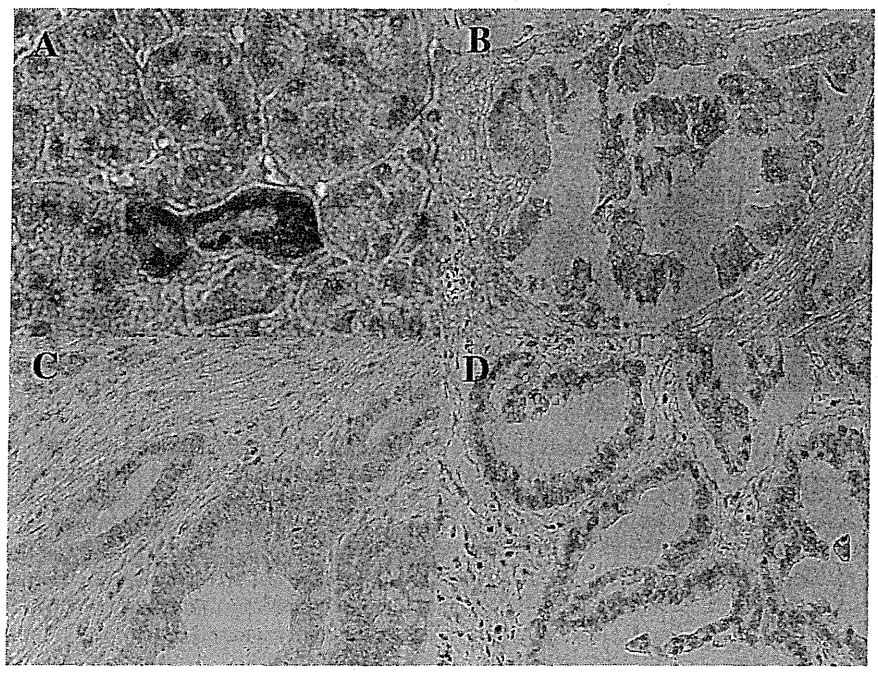

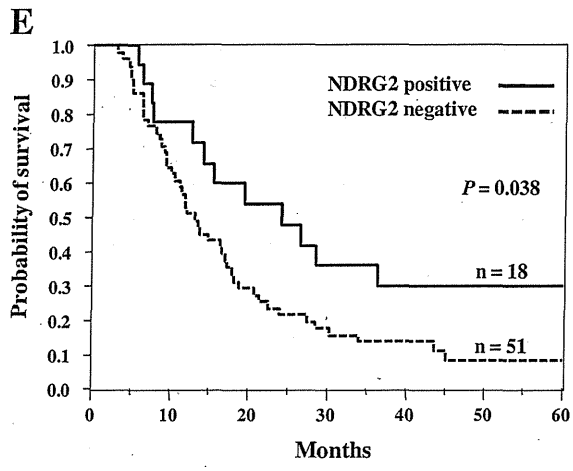

Fig. 1. (A)–(D) Results of representative immmunohistochemical analyses of NDRG2. (A) Strong immunoreactivity was observed in the cytoplasm and plasma membranes of non-neoplastic pancreatic duct (×400 magnification), and pancreatic ductal adenocarcinoma with moderate (B), weak (C), and negative (D) staining (×200 magnification). (E) Results of the Kaplan–Meier method indicate a poor overall survival rate of pancreatic cancer patients with negative NDRG2 expression ($P = 0.038$). Solid and dotted lines denote prognoses of NDRG2-positive and -negative patients, respectively.

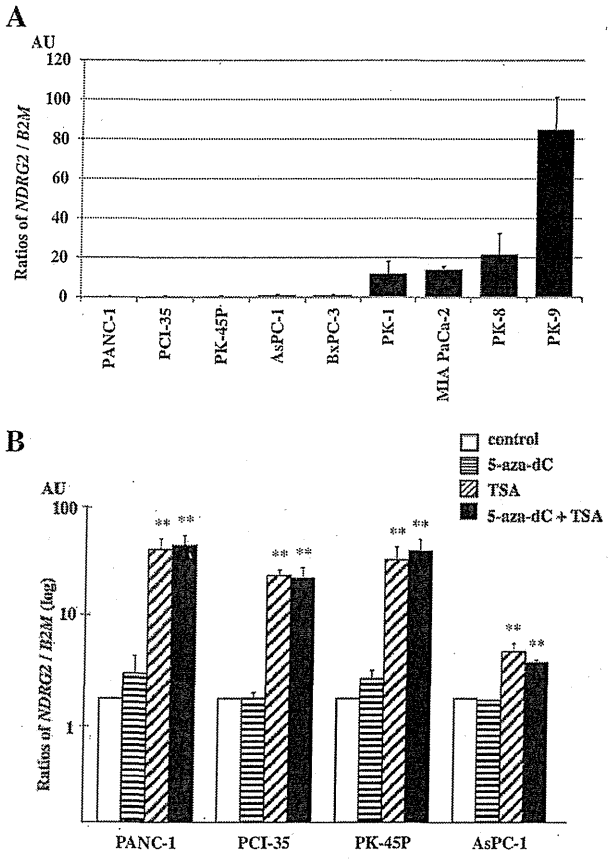

Fig. 2. Expression of *NDRG2* in human pancreatic cancer cell lines by qRT-PCR. Triplicate experiments were done, and the relative expression levels were normalized by the control *B2M* expression (arbitrary units, AU). (A) Results of 9 pancreatic cancer cells are shown. (B) Results of the four low-expressing cells are shown after 5-aza-dC and/or TSA treatments. TSA treatment up-regulated *NDRG2* expression. $^{**}P < 0.01$.

quently, cells were treated with 1 μM 5-aza-dC or 1 μM TSA (Wako, Osaka, Japan) for another 24 h. In TSA only treatment, 2×10^6 cells were plated in a 100 mm dish, and 1 μM TSA was added and cultured for 24 h. All these cells were harvested for qRT-PCR analysis.

2.7. Methylation specific PCR (MSP)

Each aliquot of 2 μg genomic DNA was modified with sodium bisulfite using an Epitect Bisulfite Kit (Qiagen) according to the manufacturer's instructions. The nucleotide sequences of primers for MSP are shown in Table 2. MSP analyses were done by methods described previously [31], and the PCR products were analyzed on 3% agarose gels. Clone A (low *NDRG2* expressing cell line) and LS174T (high *NDRG2* expressing cell line) were used as methylated and unmethylated control cells, respectively.

2.8. Statistical analysis

The Chi-square test was used to examine the correlation between *NDRG2* expression and clinicopathological factors. Survival curves were plotted using the Kaplan–Meier product-limit method, and differences between survival curves were tested using the log-rank test. The gene expression levels before and after 5-aza-dC and/or TSA treatments were analyzed by *t*-test. These statistical analyses were calculated using JMP v9.0 software (SAS Institute Inc., Cary, NC), and results were considered statistically significant when $P < 0.05$.

3. Results

3.1. NDRG2 negative staining correlated with poor prognosis in primary pancreatic cancer

We investigated the expression level of NDRG2 in surgically resected paired cancerous and corresponding normal tissues by immunohistochemical examination. Typical examples are shown in Fig. 1A–D. The spatial distribution of NDRG2 was mainly confined to the cytoplasm and plasma membrane with moderate to strong staining in noncancerous pancreatic ductal cells (Fig. 1A). According to the immunohistochemical results, of the 69 pancreatic cancer specimens examined, one exhibited a moderate NDRG2 expression in tumor cells (Fig. 1B), 17 specimens were weak (Fig. 1C), but no tumor showed stronger NDRG2 expression than normal tissue. The remaining 51 tumors were negative, as shown in Fig. 1D. One moderate and 17 weakly staining tumors were categorized as positive NDRG2 staining (18/69, 26.1%), and 51 tumors (73.9%) were negative. No significant associations were observed in clinicopathological features between positive and negative staining groups (see Table 1). However, the Kaplan–Meier analysis indicated a significant association ($P = 0.038$) between poor prognosis and negative NDRG2 expression in pancreatic cancer patients (Fig. 1E).

3.2. Restoration of NDRG2 expression after 5-aza-dC and/or TSA treatment

To determine whether epigenetic silencing contributes to suppression of the *NDRG2* transcription, we analyzed *in vitro* studies using pancreatic cancer cell lines. The mRNA expressions of *NDRG2* in 9 pancreatic cancer cell lines were determined by

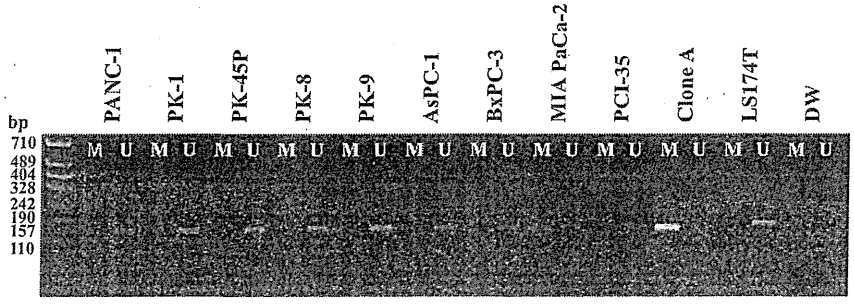

Fig. 3. MSP analyses in pancreatic cancer cell lines. Results of methylation- and unmethylation-specific PCR are indicated by M and U, respectively. All of the cell lines showed unmethylation with one exception: MIA PaCa-2 was partially methylated.

qRT-PCR analyses and found that different cell lines showed different levels of *NDRG2* expression (Fig. 2A). PANC-1, PCI-35, PK45P, AsPC-1 and BxPC-3 showed strong repression, and relatively high expression was observed in PK-9. Results of Western blot analyses correlated well with those of qRT-PCR (data not shown). We selected four pancreatic cancer cell lines (PANC-1, PCI-35, PK45P and AsPC-1) with strong repression of NDRG2 for further analyses. These cells were treated with a demethylating agent, 5-aza-dC, and/or a histone deacetylase (HDAC) inhibitor, TSA; results are shown in Fig 2B. Although no increased *NDRG2* expression was observed after the 5-aza-dC treatment alone, TSA treatment significantly up-regulated *NDRG2* expression. These results suggest that histone modification is one of the main causes for the decreased *NDRG2* expression.

3.3. Promoter hypermethylation was not involved in the decreased NDRG2 expression

It has been reported that hypermethylation is one of the main cause of suppressed expression of *NDRG2* in glioblastoma [7], meningioma [8], hepatocellular carcinoma [9], colorectal cancer [13] and oral squamous-cell carcinoma [16]. We also analyzed other types of cancer cell lines using bisulfite modified sequencing analyses and found that colon cancer cell lines Clone A and LS174T showed methylated and unmethylated CpG islands, respectively (data not shown). Using these cell lines as controls, we studied the methylation status in pancreatic cancer. All the pancreatic cancer cell lines were unmethylated except for MIA PaCa-2, which was partially methylated (Fig. 3). We further analyzed MSP using paired resected normal and cancerous pancreatic tissues from 22 pancreatic cancer patients. As expected, all of the specimens showed the unmethylated pattern, although one was partially methylated (data not shown). These results suggest that the transcriptional repression of *NDRG2* does not mainly depend on hypermethylation.

4. Discussion

Pancreatic cancer is a highly malignant gastrointestinal tumor. Only surgery with adjuvant chemotherapy can achieve a long-term perspective in patients with localized tumors. However, even under optimal treatment conditions, the 5-year survival rate do not exceed 25% [32]. To improve that situation, investigation of new therapeutic agents for pancreatic cancer treatment is essential.

Recently, an accumulation of evidence has indicated that the *NDRG2* gene downregulated in various cancers. In pancreatic cancer, however, little evidence has been reported [10], and no study on an association with prognosis has been reported to date. We demonstrated that NDRG2 expression was significantly reduced and found a significant association between poor prognosis and suppressed expression in pancreatic cancer. As there were no differences, including chemotherapeutic status, between the NDRG2 positive and negative groups, the expression of NDRG2 is likely to be an independent prognostic factor in pancreatic cancer.

We found that histone modification is one of the main mechanisms for downregulating the *NDRG2* expression in pancreatic cancer, and no such mechanisms have previously been reported to control *NDRG2* expression. Histone modification has emerged as a critical component of an epigenetic indexing system demarcating transcriptionally active chromatin domains. In general, while increased histone acetylation is associated with open and active chromatin and increased transcription, deacetylated histones are associated with condensed chromatin and transcriptional repression [33]. Histone deacethylases (HDACs) remove acethyl groups from histones, thereby inducing chromatin condensation and transcriptional repression [34]. Eighteen HDACs have been identified in humans, and they are subdivided into four classes based on their homology to yeast HDACs, their subcellular localization and their enzymatic activities [35]. In pancreatic cancer, high HDAC I expression together with HIF1α were associated with poor prognosis in a series of 39 pancreatic carcinomas [36]. Class I- and class II-selective HDAC inhibitors both synergize in inducing growth arrest and death of pancreatic cells [37]. Other research has also increased our understanding of HDAC function in pancreatic cancer [38]. At least 12 different HDAC inhibitors are undergoing clinical trials as monotherapies or in combination with other adjuvant therapies such as retinoic acid, paclitaxel, gemcitabine, or radiation in patients with various hematologic and solid tumors of the lung, breast, kidney, or bladder as well as with melanoma, glioblastoma, leukemia, lymphomas, and multiple myeloma [39,40]. In pancreatic cancer, promising results have been shown using suberoylanilindehydroxamic acid (SAHA), butyrate, and some other HDAC inhibitors in experimental studies [38,41]. TSA induced G2 arrest and apoptosis in human pancreatic cancer cell lines with mutated TP53 by induction of CDKN1A [42]. Synergistic enhancement of the cytotoxicity of TSA with proteasome inhibitor has also been reported [43]. Our present results that *NDRG2* expression is suppressed mainly by histone-mediated mechanisms and that suppression of *NDRG2* correlates with poor prognosis may provide some valuable clues for the clinical management of patients with pancreatic cancer utilizing a HDAC inhibitor.

The present study indicates that *NDRG2* is likely to be a tumor suppressor gene, reinforcing the data previously reported. In addition, we have demonstrated that inactivation of *NDRG2* associates with poor prognosis in pancreatic cancer. Furthermore, we conclude that epigenetic silencing, such as histone modification, might be the major cause of the frequent loss of NDRG2 expression. Further studies elucidating NDRG2 function will provide a unique and powerful tool for developing novel and useful applications for diagnosis and treatment of patients with pancreatic cancer.

Acknowledgments

We are grateful to Dr. Barbara Lee Smith Pierce (University of Maryland University College) for editorial work in the preparation of this manuscript, to Naomi Kanai, Emiko Kondo, Emiko Shibuya, Midori Chiba, and Keiko Inabe for excellent technical assistance, and to Biomedical Research Core (Tohoku University School of Medicine) for technical support. This work was supported in part by Grants-in-Aid (Grant #17015003, 22591512, and 23590452) and by the Academic Frontier Project for Private Universities: matching fund subsidy 2006–2010 from the Ministry of Education, Culture, Sports, Science and Technology of Japan, a Grant-in-Aid for Cancer Research (Grant #18–19) from the Ministry of Health, Labour and Welfare of Japan, Pancreas Research Foundation of Japan, and Gonryo Medical Foundation.

References

[1] R. Siegel, D. Naishadham, A. Jemal, Cancer statistics, CA Cancer J. Clin. 62 (2012) (2012) 10–29.

[2] M. Ducreux, V. Boige, D. Goere, E. Deutsch, P. Ezra, D. Elias, D. Malka, The multidisciplinary management of gastrointestinal cancer. Pancreatic cancer: from pathogenesis to cure, Best Pract. Res. Clin. Gastroenterol. 21 (2007) 997–1014.

[3] S. Boulkroun, M. Fay, M.C. Zennaro, B. Escoubet, F. Jaisser, M. Blot-Chabaud, N. Farman, N. Courtois-Coutry, Characterization of rat NDRG2 (N-Myc downstream regulated gene 2), a novel early mineralocorticoid-specific induced gene, J. Biol. Chem. 277 (2002) 31506–31515.

[4] Y. Deng, L. Yao, L. Chau, S.S. Ng, Y. Peng, X. Liu, W.S. Au, J. Wang, F. Li, S. Ji, H. Han, X. Nie, Q. Li, H.F. Kung, S.Y. Leung, M.C. Lin, N-Myc downstream-regulated gene 2 (NDRG2) inhibits glioblastoma cell proliferation, Int. J. Cancer 106 (2003) 342–347.